

RQT

NASA CONTRACTOR
REPORT

NASA CR-137875
MAY 1976

NASA CR-137875

(NASA-CR-137875) SPACECRAFT RECEIVING
ANTENNA STUDY: OUTER PLANETS ATMOSPHERIC
ENTRY PROBE (McDonnell-Douglas Astronautics
Co.) 60 p HC A04/MF A01 CSCL 09C

N77-31354

Unclas
47022

G3/32

SPACECRAFT RECEIVING ANTENNA STUDY

Outer Planets Atmospheric Entry Probe

By E.A. Kublman



Prepared by

MCDONNELL DOUGLAS ASTRONAUTICS COMPANY — EAST

St. Louis, Missouri 63166 (314) 232-0232

for Lewis Research Center

Moffett Field, California 94035

SPACECRAFT RECEIVING ANTENNA STUDY

Outer Planet Atmospheric Entry Probe

By E. A. Kuhlman

Distribution of this report is provided in the interest of information exchange. Responsibility for the contents resides in the author or organization that prepared it.

Prepared Under Contract No. 2-9027 by

MCDONNELL DOUGLAS ASTRONAUTICS COMPANY – EAST

Saint Louis, Missouri

for

AMES RESEARCH CENTER

NATIONAL AERONAUTICS AND SPACE ADMINISTRATION

TABLE OF CONTENTS

TABLE OF CONTENTS	iii
LIST OF FIGURES	v
LIST OF TABLES	vii
SUMMARY	1
INTRODUCTION	3
ANTENNA DESIGN	5
Candidate Antenna Designs	5
Lindenblad antenna	6
Conical spiral antenna	6
Loop-vee antenna	7
Quadrifilar helix antenna	7
Antenna Selection	7
MODEL ANTENNA TESTS	13
Test Antenna	13
Test Setup	14
Test Configurations	15
Configuration No. 1	15
Configuration No. 2	15
Configuration No. 3	15
Configuration No. 4	15
Test Results	15
Radiation patterns	15
Impedance	16
Bandwidth	16
CONCLUSIONS	53
REFERENCES	55
ACKNOWLEDGEMENTS	57

MISSING
 PRECEDING PAGE ~~IS~~ NOT FILMED

LIST OF FIGURES

FIGURE

1	Lindenblad Antenna	9
2	Calculated Radiation Patterns of Lindenblad Antenna - Single Element and Two Element Array	9
3	Typical Conical Spiral Antenna	10
4	Loop-Vee Antenna	10
5	Quadrifilar Helix Antenna - 3/4 Wavelength, 3/4 Turn	11
6	Typical Radiation Pattern for a 3/4 Wavelength, 3/4 Turn Quadrifilar Helix	12
7	Model Quadrifilar Helix Antenna	17
8	Radiation Patterns with Quadrifilar Helix Elements Wrapped Around Balun Feed - 2.17 GHz	18
9	Radiation Patterns of 3/4λ-3/4 Turn Quadrifilar Helix Antenna - 2.2 GHz	20
10	VSWR of 3/4λ-3/4 Turn Quadrifilar Helix Antenna	23
11	Pioneer Spacecraft Test Configuration	23
12	Coordinate System for Antenna Pattern Measurements	24
13	Model Spacecraft Support Fixture for Radiation Pattern Measurements	25
14	Basic Spacecraft Test Configuration	26
15	Antenna Extended Axially Aft of Position for Basic Test Configuration	27
16	Antenna Position Rotated 22.5° Relative to Basic Test Configuration	28
17	Antenna Extended Axially Aft for Rotated Position	29
18	Radiation Patterns for Test Configuration No. 1 - 2.2 GHz	30
19	Radiation Patterns for Test Configuration No. 2 - 2.2 GHz	35
20	Radiation Patterns for Test Configuration No. 3 - 2.2 GHz	40
21	Radiation Patterns for Test Configuration No. 4 - 2.2 GHz	45
22	VSWR of Antenna Mounted on Spacecraft	50
23	Radiation Patterns for Bandwidth Evaluation - 2.0 GHz	51
24	Radiation Patterns for Bandwidth Evaluation - 2.3 GHz	52

LIST OF PAGES

Title Page

ii thru viii

i thru 57

~~RECEIVING PAGE BLANK NOT FILMED~~

LIST OF TABLES

I	Antenna Characteristics	8
II	Maximum Pattern Dissymmetry (dB)	16
III	Maximum Axial Ratio (dB)	16

~~PREVIOUS PAGE BLANK NOT FILMED~~

SUMMARY

As a result of trade-off and selection studies, a quadrifilar helix antenna was selected for the Pioneer spacecraft receiving antenna. A model was constructed for radiation pattern measurement at 2.2 GHz (550 MHz full scale). The pattern symmetry is within 1 dB from the zenith ($\theta = 0^\circ$) to 10° above the equatorial plane ($\theta = 80^\circ$). Above $\theta = 90^\circ$ the pattern symmetry and axial ratio degrade slowly. Over this same region the axial ratio varies from 0 to 1.5 dB. It is believed that further improvement could only be obtained with precision tooling.

Radiation patterns were measured with the model quadrifilar helix antenna mounted on a Pioneer spacecraft model. Four different configurations were tested. The results show that the antenna location does not have a major effect on its patterns over the aft hemisphere ($\theta = 0^\circ$ to $\theta = 90^\circ$). However, moving the antenna away from the spacecraft improves the antenna performance from $\theta = 90^\circ$ to $\theta = 110^\circ$. Measurements were also made to evaluate the effect of the spacecraft on the VSWR and bandwidth of the antenna and found to be very minor. The peak circular gain of the quadrifilar helix antenna should be about 2.2 dB based on an expected efficiency of 71% (-1.5 dB) for a full scale antenna.

Radiation patterns and VSWR plots are given to demonstrate the performance of the antenna in the various test configurations.

INTRODUCTION

The radiation patterns of the spacecraft receiving antenna are an important item in the design of the Outer Planets Probe (OPP) communications link. Since the Pioneer spacecraft spins about its roll axis, an axially-symmetric receiving antenna pattern is required for best link stability. For maximum link power transfer, circular polarization (with same sense as probe transmitting) and proper radiation pattern distribution are required. The latter is a function of the spacecraft and probe trajectories. If the range of look angles (relative to spacecraft) is small and near the equatorial plane of the spacecraft, two elements can be arrayed to increase the gain in the desired region. This would also have an added benefit by increasing the noise rejection in the null region. However, if the range of look angles is large a single radiation element is probably required. In this case, the control of the radiation pattern distribution is limited.

The objective of this task (Task 4.1.2) is to select and test an antenna which has an axially symmetric radiation pattern with the pattern beam oriented to cover a spacecraft look angle region defined by a Jupiter mission.

The study approach consisted of selecting an antenna design from a number of candidate designs, constructing a 1/4-scale model of the antenna, and then measuring radiation patterns with the antenna appropriately mounted on a 1/4-scale Pioneer spacecraft model at several feasible locations. The Pioneer model was provided by NASA-ARC and was updated to include equipment required for a Jupiter mission prior to delivery to MDAC-E.

This report describes the selected antenna design, the configurations tested, and gives the test data necessary to evaluate effects of the spacecraft on the antenna radiation pattern and the performance of that antenna relative to OPP missions.

~~PRECEDING PAGE BLANK NOT FILLED~~

ANTENNA DESIGN

This section describes the candidate antenna designs and discusses the selection of a receiving antenna design for a spin spacecraft during the post entry communications period.

Candidate Antenna Designs

The primary radiation pattern requirements selected for the spacecraft receiving-antenna (Table 19, Reference 1) are as follows:

- a. Roll Planes
 - o Pattern Symmetry - 1 dB peak to peak (goal)
- b. Elevation Planes
 - o Beamwidth - 79.2°
 - o Beam Center - 39.6°
 - o Spacecraft View Angles - $\theta = 32.5$ to 96.5°
(Note: $\theta = 0^\circ$ at zenith)
- c. Polarization
 - o Circular

Other antenna factors of importance are gain and efficiency. However, these are largely dependent upon the antenna type selected. The frequency used for this study was 550 MHz.

Antenna types which are circularly polarized and have essentially axially symmetric patterns include the following:

- a. Lindenblad
- b. conical spiral
- c. loop-vee
- d. quadrifilar helix

A brief review of other antenna types did not identify a potential candidate which had performance characteristics preferable to those cited above. Therefore, those listed above were the only candidate designs given serious consideration. The primary items of consideration in the antenna selection trade study were the antenna radiation pattern characteristics, pattern isolation from spacecraft structure and size. Other items of consideration such as pattern control feasibility, implementation feasibility, compatibility with spacecraft systems, weight and complexity were given only minor consideration except where they were obviously important as factors in the choice between two otherwise equal candidates.

~~RECEIVING~~-PAGE BLANK NOT FILMED

Lindenblad antenna. - The single element Lindenblad antenna (Figure 1) has a circularly polarized radiation pattern with a beamwidth of about 80° which is normal to the antenna axis. The pattern in any elevation plane can be approximated by:

$$E(\theta) = \sin^{1.3} \theta$$

where $\theta = 0^\circ$ is coincident with the antenna axis. The pattern is axially-symmetric in any azimuth conic plane. The peak directivity for this pattern is 2.10 dB. For a uniform (omnidirectional) opposite sense polarization level of -20 dB, the directivity would be reduced about 0.07 dB. At the initial spacecraft view angle ($\theta = 32.5^\circ$), the directivity of a Lindenblad antenna would be -5.91 dB, about 9.7 dB below that required (Reference 1). Lindenblad elements can be arrayed and phased to point the beam off broadside. This would be expected to narrow the beam and increase the gain. However, as the beam is scanned off the normal, a sidelobe starts to emerge which reduces the directivity of the main beam. The gain at $\theta = 32.5^\circ$ (spacecraft look angle) for fixed beam angles 30 and 41.8° off broadside (δ phase = 90° and 120° respectively) is essentially the same as that for the single Lindenblad element. Figure 2 shows calculated elevation patterns for a single element and two elements arrayed with the phase differences cited above. More elements could be added to suppress the side lobes, but this would result in an even narrower beamwidth and would likely require active beam direction control.

The volume required for a single Lindenblad element at 550 MHz is essentially a cylinder 33.5 cm (13.2 in.) in diameter and 19.3 cm (7.6 in.) in length. The weight would not be a significant factor, but the complexity and cantilevered elements could be expected to result in numerous implementation problems associated with shock and vibration requirements.

Therefore, since the Lindenblad antenna radiation pattern gain is well below (approximately 9.7 dB) that of the ideal antenna radiation pattern characteristics (Reference 1) and as its mechanical design is not ideal, it was rejected as a viable candidate for the spacecraft receiving antenna.

Conical spiral antenna. - A review of the radiation pattern characteristics of the conical spiral antenna (Figure 3) indicates that the pattern symmetry is on the order of 3 dB peak to peak. The dissymmetry is due, in part, to the broad band characteristics of the conical spiral. It is possible, however, that additional development could improve the pattern symmetry. The radiation pattern shape is similar to a loop-vee. In an elevation plane the beamwidth is about 55° centered approximately $\theta = 60^\circ$. The peak circularly polarized gain is about 3 dB. The angle at which the pattern peak occurs and the beamwidth can be altered to some extent by altering the cone angle and the pitch angle of the element windings. However, the pattern symmetry is expected to vary as the spiral arm geometry changes.

The volume required (estimated) is essentially a cone with a base diameter

Loop-vee antenna. - The loop-vee antenna (Figure 4) has previously been selected as the spacecraft receiving antenna (Reference 2). Details of the loop-vee antenna and its pattern characteristics are given in Reference 2 and will not be repeated here. This data indicates that the azimuthal pattern variation is about 1 dB peak to peak. Data received from Vega Precision Laboratories Incorporated pertaining to their Model 837S loop-vee antenna indicates that peak to peak azimuthal variations of 2 to 2 1/2 dB can be expected. Other private discussions of the loop-vee antenna capabilities indicated that the radiation pattern of the loop-vee antenna is strongly influenced by the physical environment. This appears to be due to the required balance between the horizontally polarized component of the loop and the vertically polarized component of the vertical "vee" elements. The addition of dielectric members (Reference 2) required to stabilize the four vertical and loop segment members may affect the symmetry of the pattern.

A comparison of the loop-vee radiation pattern (Reference 2) with an idealized Gaussian pattern (Table 32 of Reference 1) shows that the loop-vee has a negative margin of -3.29 dB at $\theta = 32.5^\circ$ and positive margin of 3.05 dB at $\theta = 96.5^\circ$.

The volume required for the loop-vee antenna at 550 MHz is essentially a cylinder 22.9 cm (9.0 in.) in diameter and 19.1 cm (7.5 in.) in length.

Quadrifilar helix antenna. - The quadrifilar helix antenna can take numerous forms (References 3 thru 9). Of these $3/4 \lambda - 3/4$ turn version (Reference 9) was selected as a spacecraft receiving antenna candidate. Figure 5 shows a sketch of this antenna configuration. The radiation patterns of a $3/4 \lambda - 3/4$ turn quadrifilar helix antenna (Reference 9) have a low axial ratio and excellent pattern symmetry. This antenna may also be arrayed to control the elevation pattern shape as demonstrated by a two element array design described and supported by test data in Reference 9. Data from an array of two elements (Reference 9) shows a main beam symmetry of 1 dB peak to peak or less. Comparison of the expected radiation pattern (Figure 6), using the calculated directivity and an estimated efficiency of -1.5 dB (71%), with the required pattern (Reference 1) shows a positive performance margin of .09 dB at $\theta = 32.5^\circ$ and 1.51 dB at $\theta = 96.5^\circ$.

The volume required for this antenna is a cylinder 6.1 to 7.6 cm (2.4 to 3.0 in.) in diameter and 38.6 cm (15.2 in.) long.

Antenna Selection

The parameters used to evaluate and compare the performance of the candidate antennas are summarized in Table I.

The Lindenblad antenna radiation pattern directivity is well below (approximately 9.7 dB) that of the ideal antenna radiation characteristics. Calculations for two element arrays did not show any improvement. Further,

TABLE I
ANTENNA CHARACTERISTICS

CANDIDATE ANTENNA	GAIN MARGIN PERFORMANCE (dB)	PATTERN SYMMETRY (dB)	VOLUME (IN. ³)	REMARKS
LINDENBLAD	-9.7	***	1040	UNDESIRABLE, MECHANICAL DESIGN
CONICAL SPIRAL	**	3	2268	LARGE VOLUME
LOOP-VEE	-3.3	2-3	477	SENSITIVE TO PHYSICAL LOCATION
QUADRIFILAR HELIX	0.1	1	107	COMPACT

*COMPARED TO IDEAL RADIATION PATTERN REQUIREMENT (REFERENCE 1)
AT $\theta = 32.5^\circ$ - GAIN = $10 \text{ LOG}_{10} \{1.5804 \text{ EXP} - 1/2 [0.0297 (\theta - 39.6^\circ)]^2\}$

**NOT EVALUATED BUT GAIN AT $\theta = 32.5^\circ$ APPEARS TO BE COMPARABLE TO LOOP-VEE ANTENNA

***NO AZIMUTH PATTERN DATA AVAILABLE

the mechanical design of the Lindenblad antenna is somewhat unwieldy and it appears would present a number of implementation problems associated with shock and vibration requirements.

The conical spiral is very large relative to the other candidate antenna designs. Therefore, since the antenna pattern does not have superior axial symmetry and axial ratio and the broad bandwidth capability is not required, the conical spiral was rejected as the spacecraft receiving antenna.

The loop-vee antenna pattern is sensitive to its physical environment and has limited pattern control capability. Changes in the ground plane, for example, would require changes in the radiating element configuration to regain the balance between horizontal and vertical components required for low axial ratio of the radiation patterns. Further, the available data did not indicate that axially-symmetric patterns equivalent to those expected for the quadrifilar helix antenna could be achieved. In addition, the expected pattern of the loop-vee antenna (Reference 2) does not meet the requirements established for an ideal antenna shape and directivity. Therefore, based on the above factors, the loop-vee antenna design was rejected as the spacecraft receiving antenna design.

The $3/4 \lambda - 3/4$ turn quadrifilar helix antenna was selected from the candidate antenna designs as the spacecraft receiving antenna. Radiation pattern symmetry, low axial ratio, and control potential were considered superior to the competing designs. Its expected pattern and directivity equal or exceed the requirements established for an ideal antenna pattern shape and directivity. In addition, the quadrifilar helix antenna is compact and a resonant version has been successfully designed to meet the physical environment of the Viking Orbiter (Reference 10).

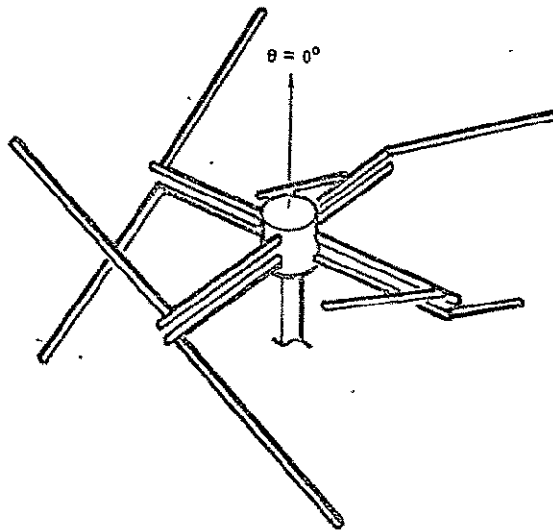


FIGURE 1
LINDENBLAD ANTENNA

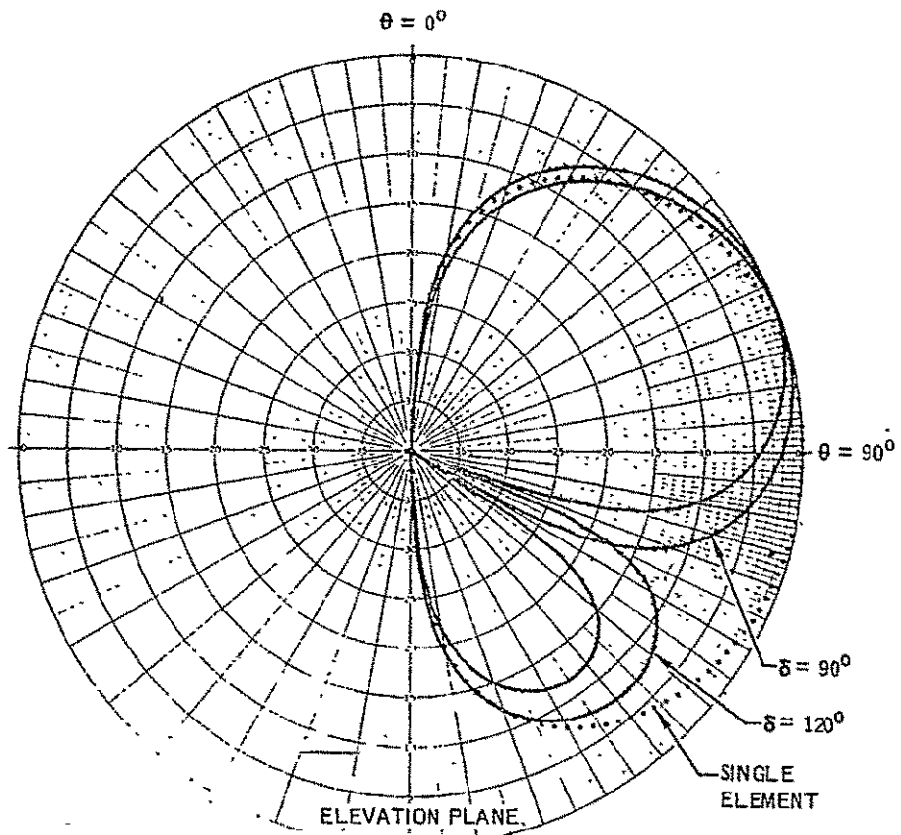


FIGURE 2
CALCULATED RADIATION PATTERNS OF LINDENBLAD ANTENNA -
SINGLE ELEMENT AND TWO ELEMENT ARRAY

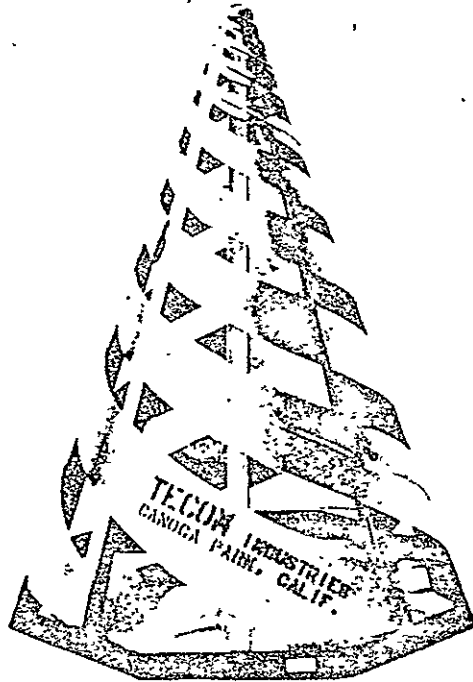


FIGURE 3
TYPICAL CONICAL SPIRAL ANTENNA

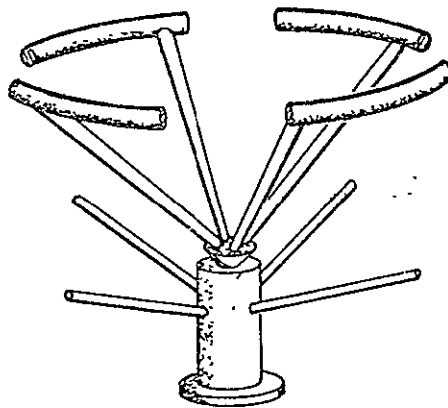


FIGURE 4
LOOP-VEE ANTENNA

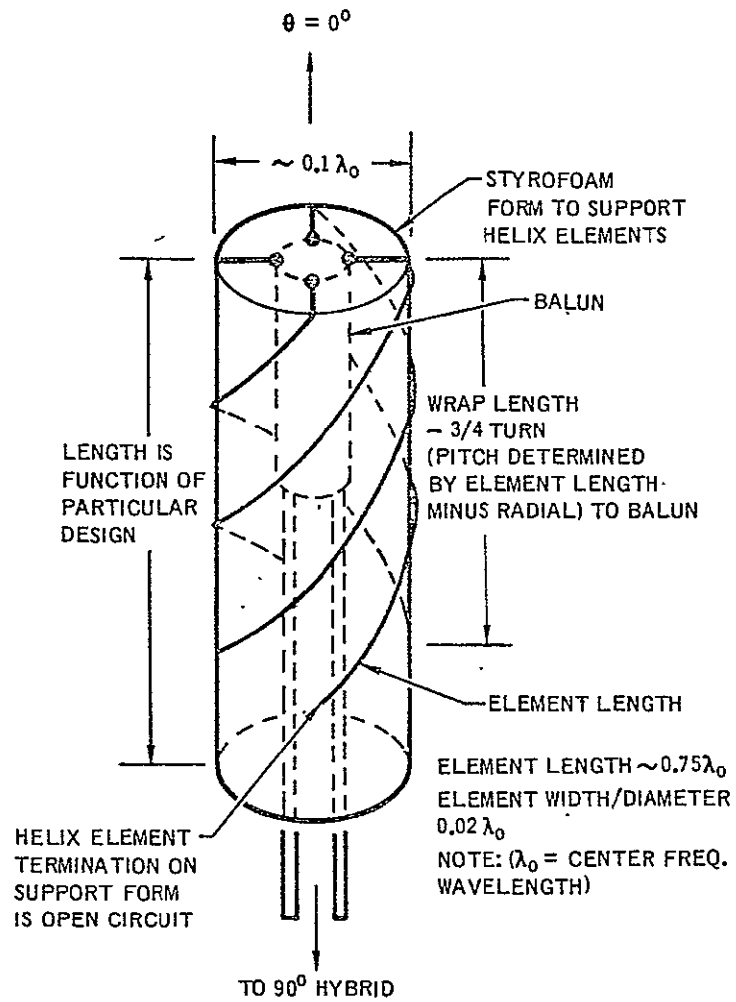
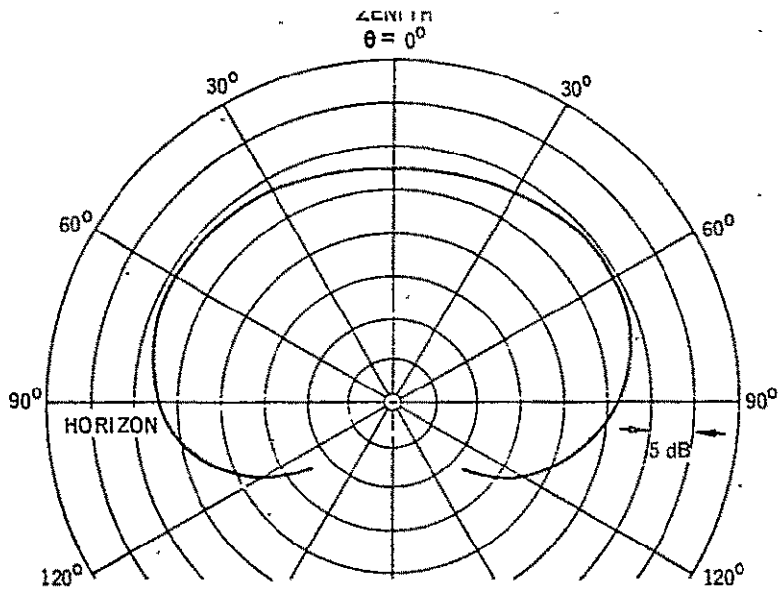


FIGURE 5
QUADRIFILAR HELIX ANTENNA -
3/4 WAVELENGTH, 3/4 TURN



NOTE: FIG 3, REFERENCE 9

FIGURE 6

**TYPICAL RADIATION PATTERN FOR A 3/4 WAVELENGTH,
3/4 TURN QUADRIFILAR HELIX**

MODEL ANTENNA TESTS

This section describes the test antenna, test setup, test configurations and test results. The test procedures used are standard practice and, therefore, will not be explained in this report.

Test Antenna

A 1/4 scale model of a 3/4 wavelength 3/4 turn quadrifilar helix antenna was constructed as shown in Figure 7. The design is based on the work of Kilgus and Domer (References 5 and 9). The helix elements are 1.19 mm (0.047 in.) in diameter, 10.82 cm (4.26 in.) long and are wrapped on a styrofoam core 1.52 cm (0.60 in.) in diameter with a wrap length of 9.47 cm (3.73 in.). In this configuration the helix elements are 0.79 wavelengths long and are wrapped around the core over 3/4 turn but less than 1 turn. The four helix elements are fed with a pair of baluns fed from a 90° hybrid to obtain the proper excitation magnitude and phase of each element. This balun design (Reference 11) is somewhat different than the folded balun approach by Domer or Kilgus. However, the end result is equivalent. The initial antenna models were made using a simple split-tube (or split-sheath) type balun (Reference 12). The split-tube balun is used frequently to feed crossed dipole and resonant half-wave quadrifilar helix (References 3 and 6) antennas. However, the required balance was not achieved and this approach was abandoned. The folded balun approach was also tried but did not produce the desired results. The impedance bandwidth of this balun is significantly less than that of the balun used.

Initially the helix elements were wrapped around the balun. However, the model balun is slightly larger than an exact 1/4 scale version of a full scale balun (550 MHz). Although the radiation patterns (Figure 8) were reasonably good, the positions of the helix elements relative to the balun and the feed transmission line were very critical and, thus, the desired symmetry did not appear achievable. Small changes only resulted in moving the degraded region of the radiation pattern to a different angular location.

To correct this apparent deficiency, the balun was removed from the region inside the quadrifilar helix elements (Reference 13) to that shown in Figure 7. After a few adjustments, which included remaking the helix elements to achieve the best uniformity possible without resorting to special tooling, almost ideal radiation patterns were obtained as shown in Figure 9. These patterns were measured using rotating linear polarization. The principal polarization of this antenna is right-hand circular and is the same as that obtained with the helix elements wrapped around the balun. The θ -plane (elevation plane) patterns ($\phi = 0^\circ$ and 90°) closely match the pattern used as a basis for evaluating the quadrifilar antenna in the previous section. The axial symmetry of the ϕ -plane patterns (azimuth plane) is within 1 dB peak to peak from $\theta = 0^\circ$ to $\theta = 80^\circ$. At $\theta = 90^\circ$ the axial symmetry is about 1.5 dB peak to peak. With special tooling, it is expected that the antenna geometry could be improved

enough to achieve an axial symmetry of 1 dB peak to peak or less. The worst axial ratio from $\theta = 0^\circ$ to $\theta = 90^\circ$ is about 2.5 dB at $\theta = 90^\circ$. From $\theta = 0^\circ$ to $\theta = 80^\circ$ the axial ratio varies from 0 dB (or very low) to about 1.5 dB. From $\theta = 90^\circ$ to $\theta = 120^\circ$ the worst axial ratio is only about 5 dB. The peak directivity (circular polarization) of the model antenna is 3.7 dB and the peak gain is 0.5 dB compared to a standard gain horn (Scientific Atlantic - SGH 1.7). The efficiency (directivity/gain) is 48% (-2.2 dB). The low efficiency is due to the increased losses of the coax used at the frequency of the model antenna designs (2.2 GHz). The efficiency at full scale (550 MHz) is expected to be about 71% (-1.5 dB) (Reference 14). With the improved efficiency the expected peak gain of a full scale antenna would be 2.2 dB.

The voltage standing wave ratio (VSWR) of the model antenna is shown in Figure 10. It was measured with an HP Network Analyzer system. The VSWR is about 1.29:1 at 2.2 GHz and improves at both higher and lower frequencies. The highest VSWR is 2.32:1 at 2.42 GHz and would be quite acceptable.

The radiation pattern and VSWR data described above demonstrates the merits of the quadrifilar helix as an axially symmetric antenna for a spacecraft receiving antenna. Both symmetry and axial ratio are excellent. Therefore, the performance of this antenna should be more than adequate to evaluate the effects of the Pioneer spacecraft on the symmetry of its radiation pattern.

Test Setup

The test setup consisted of the Pioneer spacecraft model mounted on an antenna pattern tower, Figure 11, which supports the spacecraft spin axis 7.3 m (24 ft) above the ground. Figure 12 shows the coordinate system, relative to the spacecraft, used for measuring the radiation patterns. This coordinate system corresponds to that used for the model antenna design tests and permits direct comparison of patterns with similar coordinate designations. In this test setup, the probe can be rotated about its axis to measure conical plane (or roll plane) patterns (ϕ -plane, i.e., θ fixed and ϕ variable) from $\theta = 0^\circ$ to $\theta = 180^\circ$, or it can be held in a fixed rotational position (e.g., $\phi = 0^\circ$ or $\phi = 90^\circ$) and the tower rotated to measure elevation plane patterns (θ -plane, i.e., ϕ fixed and θ variable) which include the spacecraft axis of symmetry. The radiation patterns were measured using a rotating linear polarization with a transmission distance of 11.9 m (39 ft). The VSWR was measured using a HP slotted line, a HP 415 Standing Wave Indicator and a HP 616 B Signal Generator.

The Pioneer spacecraft model was attached to the antenna tower by means of a support fixture clamped to the dish antenna (Figure 13). The circular plate just beyond the dish antenna feed mates with the antenna tower arbor plate. This mounting arrangement takes advantage of the shadowing from the dish antenna and should minimize the effects of the tower and tower head.

Test Configurations

Four antenna locations were tested which essentially bracket the range of feasible locations.

Configuration No. 1. - The basic test configuration was the quadrifilar helix antenna mounted on the Pioneer spacecraft as shown in Figure 14. This configuration places the antenna essentially at the position established for a loop-vee antenna (Reference 14) by previous studies. The outer end of quadrifilar helix antenna extends aft of the probe adapter ring 98 cm (38.6 in.) compared to 58.4 cm (23 in.) (Note: full scale dimensions) for the loop-vee antenna configuration. This antenna location places the inner end of the antenna about $1/4 \lambda$ from the junction of the tripod which supports the antenna on the spacecraft.

Configuration No. 2. - This configuration (Figure 15) consists of extending the end of the quadrifilar helix antenna to 1.42 m (56.0 in.) aft of the probe adapter ring. This keeps the antenna outside an 18° (half angle) probe launch clearance cone established in Reference 2. This configuration would be expected to produce some improvement in patterns because the reflected energy from the spacecraft would be received at a slightly lower gain level. The hardware required to extend the antenna for this configuration would increase the spacecraft weight about 0.60 kg (1.32 lbs).

Configuration No. 3. - This configuration (Figure 16) is similar to that of No. 1 with the antenna location rotated 22.5° (same radius) to place the antenna directly over one of the four tanks clustered around the probe adapter. This location provides the antenna with a different view of the spacecraft.

Configuration No. 4. - This configuration (Figure 17) extends the antenna above the adapter ring essentially the same as Configuration No. 2 but with the rotated location selected for Configuration No. 3. This configuration would increase the spacecraft weight about the same as for Configuration No. 2, about 0.60 kg (1.32 lbs).

Test Results

Radiation Patterns. - The radiation patterns of the respective test configurations are shown in Figures 18 through 21. The pattern measurement frequency was 2.2 GHz which corresponds to 550 MHz at full scale. A comparison of these patterns with the basic antenna patterns (Figure 9) shows the effects of reflections from various parts of the spacecraft. However, the pattern changes are not large enough to identify a particular spacecraft appendage (for example, the magnetometer or RTG's) or structural feature as the cause. The axial ratio changes (0 to approximately ± 2 dB) can be attributed to a general reflection level from the spacecraft of 15 to 30 dB below the directly received level. A summary of roll plane pattern dissymmetry (peak to peak) and

maximum axial ratio is given in Tables II and III for angles of $\theta = 0^\circ$ to $\theta = 110^\circ$ (i.e., θ constant and ϕ variable). At angles greater than $\theta = 110^\circ$ the pattern symmetry is significantly affected by shadowing from the spacecraft. Axial ratios of 15 to 20 dB may also be observed in this region.

TABLE II
MAXIMUM PATTERN DISSYMMETRY (dB)

CONFIGURATION NO.	ROLL PLANE PATTERN ANGLE (θ)			
	<80	90	100	110
1	1.5	2.5	5.5	9.5
2	1.0	1.5	2.0	6.0
3	2.5	2.0	6.0	8.0
4	2.0	1.5	2.0	5.5

TABLE III
MAXIMUM AXIAL RATIO (dB)

CONFIGURATION NO.	ROLL PLANE PATTERN ANGLE (θ)			
	<80	90	100	110
1	2.5	3.0	5.0	8.0
2	2.0	2.5	5.0	7
3	2.3	3.0	5.0	9
4	1.5	2.0	4.0	7.0

Impedance. - The impedance of the quadrifilar helix is not significantly affected by the spacecraft. Figure 22 shows the VSWR of the antenna mounted on spacecraft (Configuration No. 4). The VSWR is slightly lower at 2.2 GHz than that obtained with the antenna alone (Figure 11). However, when an antenna VSWR is very low, minor reflections can cause slight changes which are insignificant in terms of antenna performance.

Bandwidth. - Radiation patterns were made with the antenna mounted on the spacecraft (Configuration No. 2) to determine the pattern bandwidth. Figure 23 shows the principal plane pattern at 2.0 GHz and Figure 24 shows pattern at 2.3 GHz. Comparison of Figures 23 and 24 with Figure 20 shows that the magnitude at $\theta = 90^\circ$ decreases about 3 dB at 2.0 GHz and increases about 2 dB at 2.3 GHz. At angles from $\theta = 0^\circ$ to $\theta = 60^\circ$ the pattern magnitude remains about the same from 2.0 to 2.3 GHz. The pattern symmetry at $\theta = 90^\circ$ is about 1.5 dB peak to peak at 2.3 GHz, the same as that at 2.2 GHz. However, below 2.2 GHz the pattern dissymmetry increases to about 2.5 at 2.1 GHz and remains the same at 2.0 GHz. Below 2.0 GHz or above 2.3 GHz the axial ratio starts to exceed 3 dB at angles around $\theta = 90^\circ$. Therefore, the bandwidth, over which the axial ratio is 3 dB or less, is about 14%, well above that required for the probe to spacecraft communication link.

ORIGINAL PAGE IS
POOR QUALITY

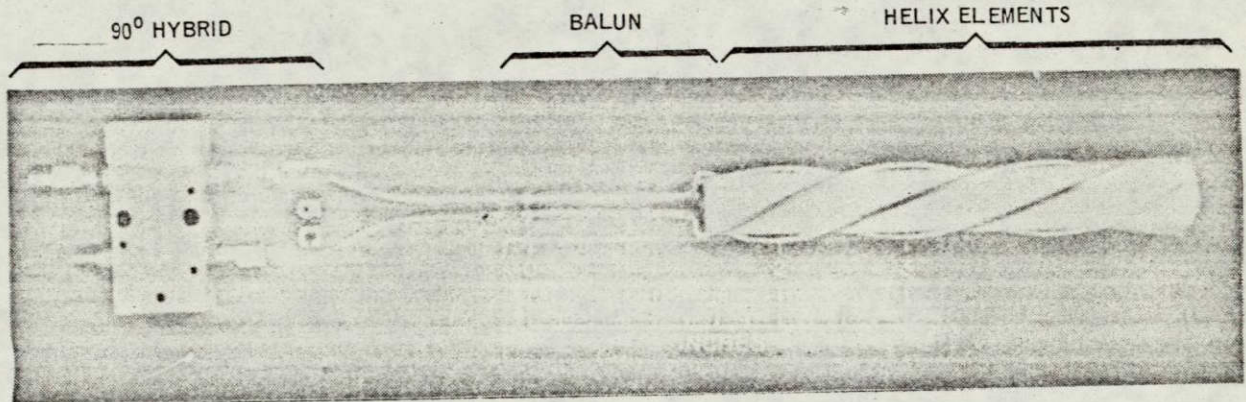


FIGURE 7
MODEL QUADRIFILAR HELIX ANTENNA

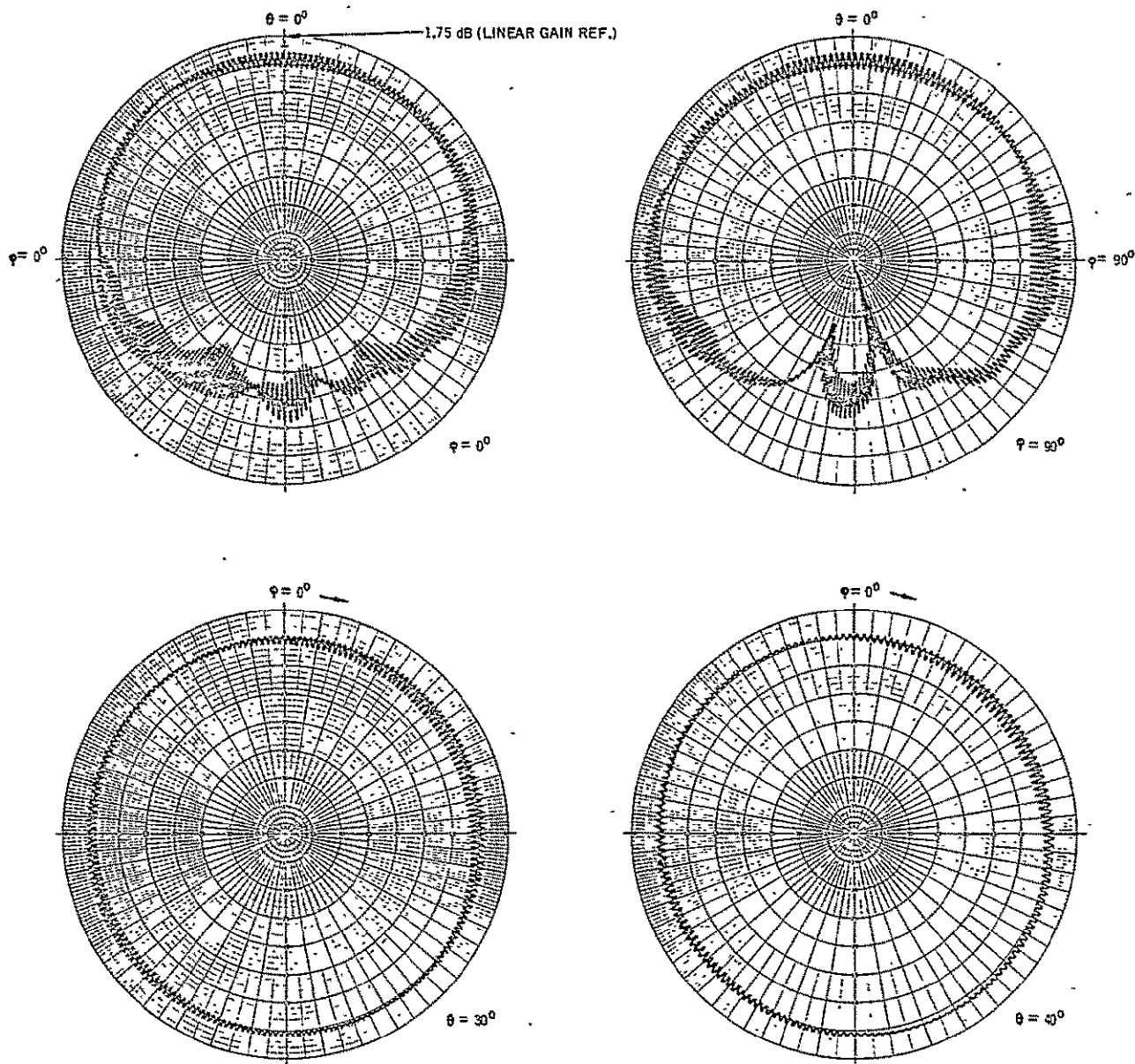


FIGURE 8

RADIATION PATTERNS WITH QUADRIFILAR HELIX ELEMENTS
 WRAPPED AROUND BALUN FEED - 2.17 GHz

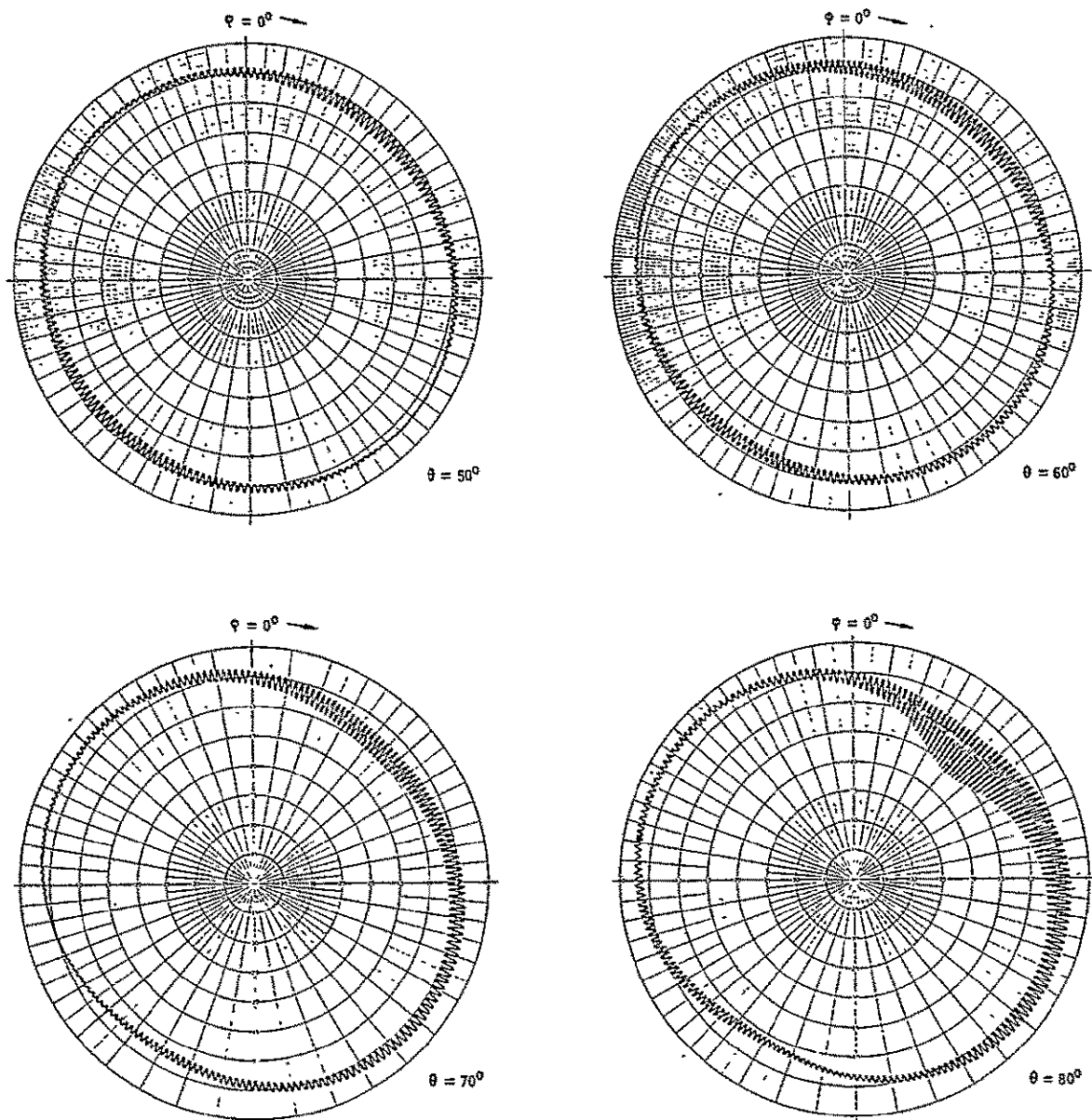


FIGURE 8 (Continued)
 RADIATION PATTERNS WITH QUADRIFOLIAR HELIX ELEMENTS
 WRAPPED AROUND BALUNFEED - 2.17 GHz

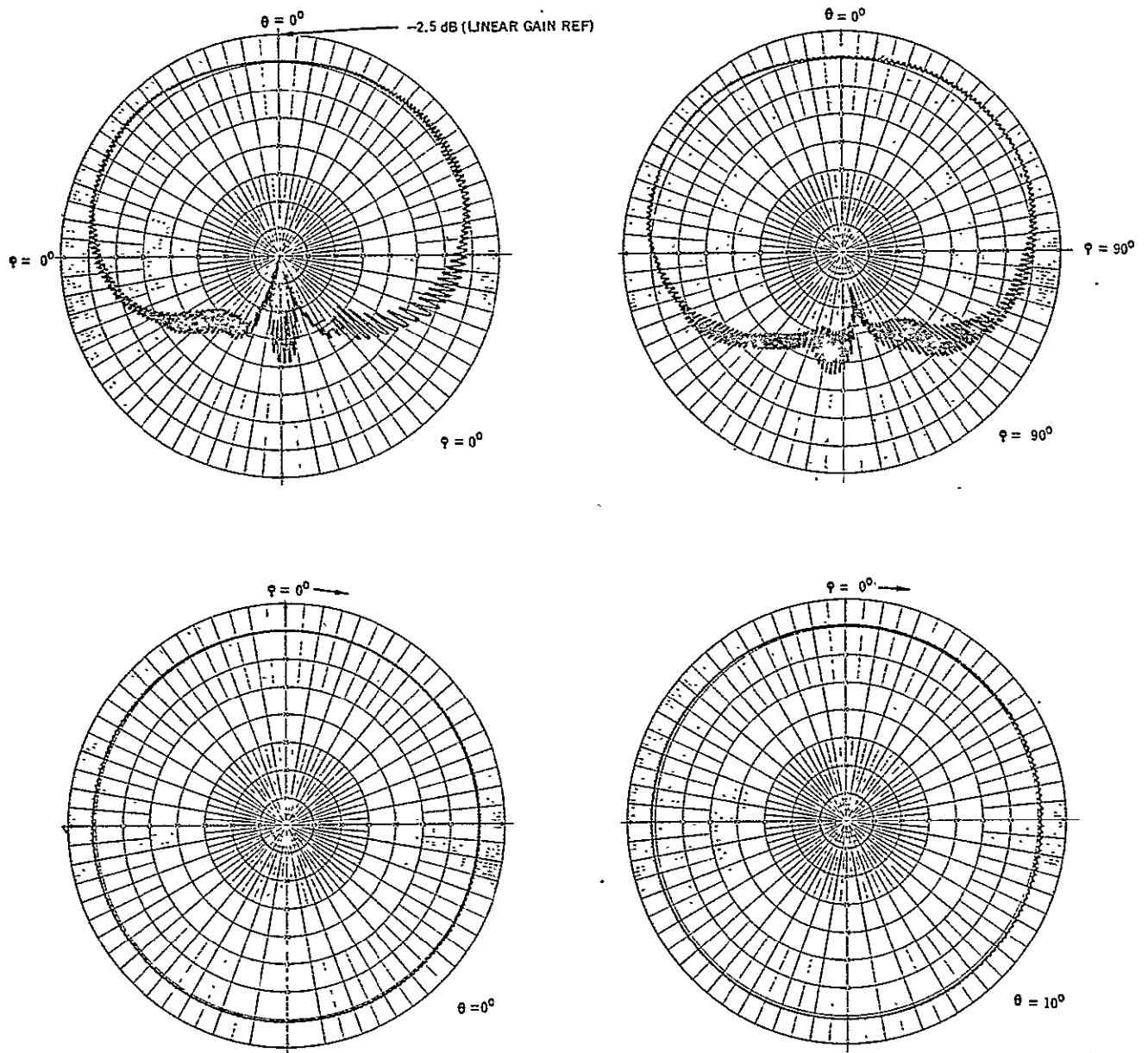


FIGURE 9

RADIATION PATTERNS OF $3/4 \lambda$ - $3/4$ TURN
 QUADRIFILAR HELIX ANTENNA - 2.2 GHz

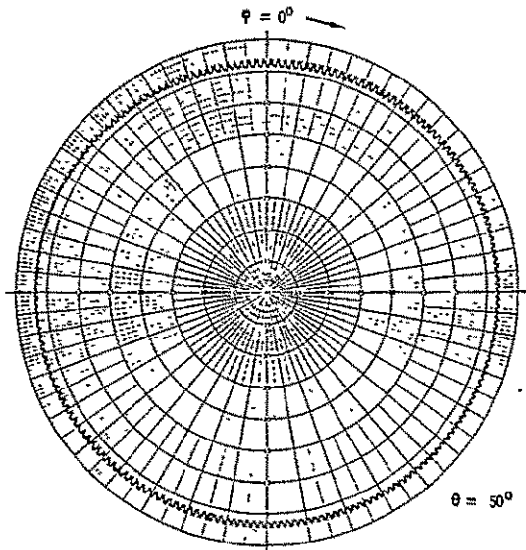
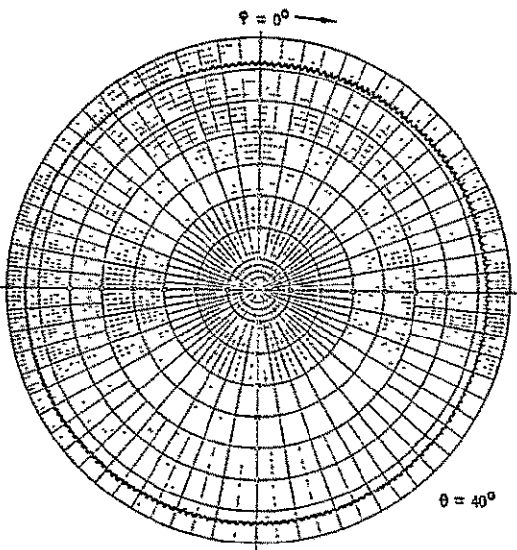
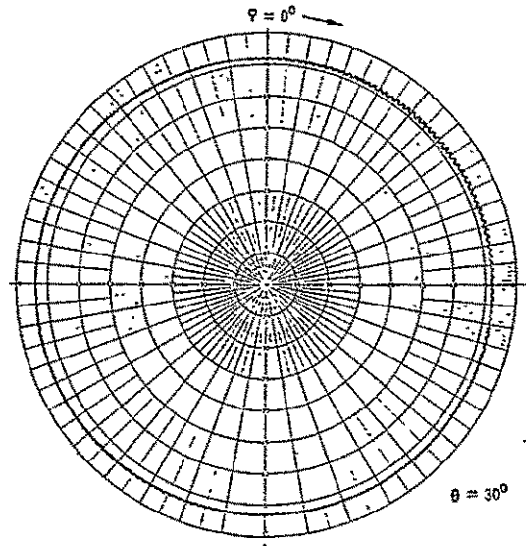
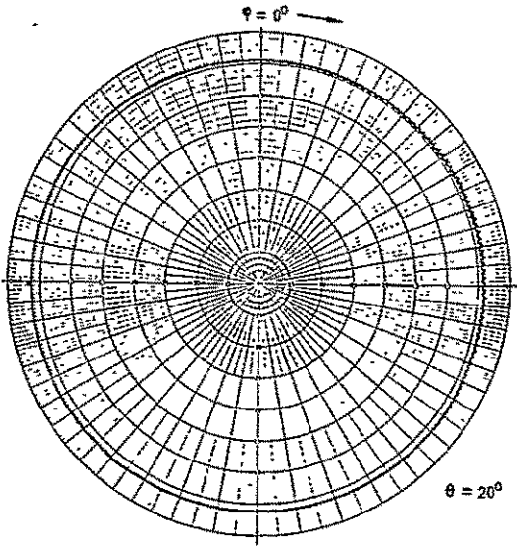


FIGURE 9 (Continued)
 RADIATION PATTERNS OF $3/4 \lambda$ - $3/4$ TURN
 QUADRIFILAR HELIX ANTENNA - 2.2 GHz

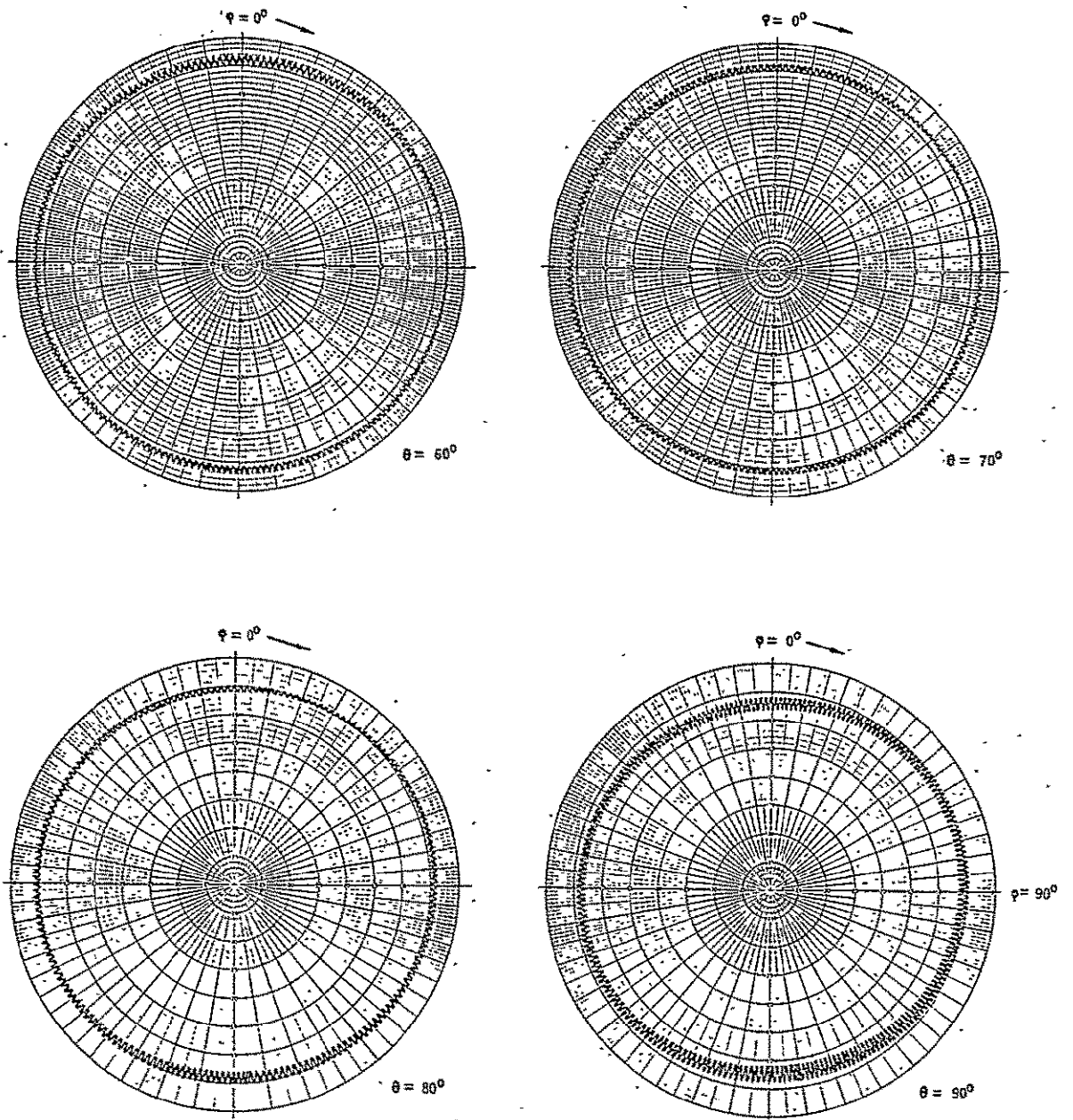
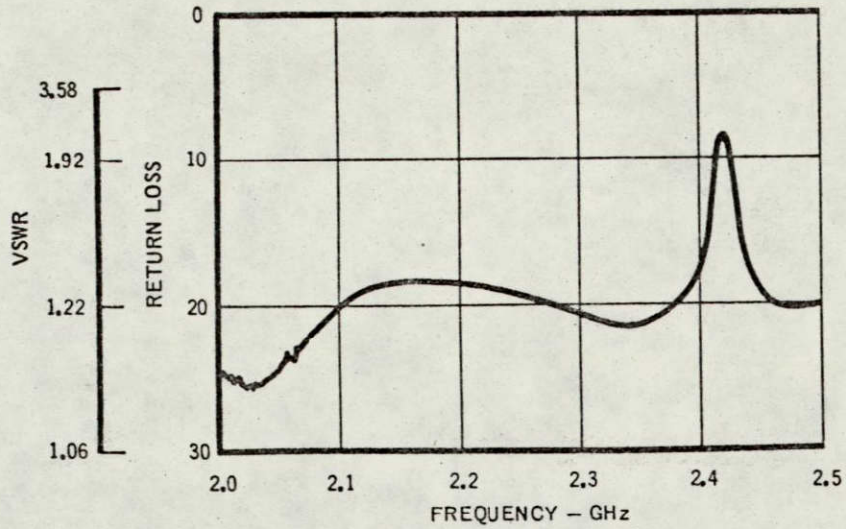


FIGURE 9 (Continued)
 RADIATION PATTERNS OF $3/4 \lambda$ - $3/4$ TURN
 QUADRIFILAR HELIX ANTENNA - 2.2 GHz



ORIGINAL PAGE IS
OF POOR QUALITY

FIGURE 10

VSWR OF $3/4\lambda$ - $3/4$ TURN QUADRIFILAR HELIX ANTENNA

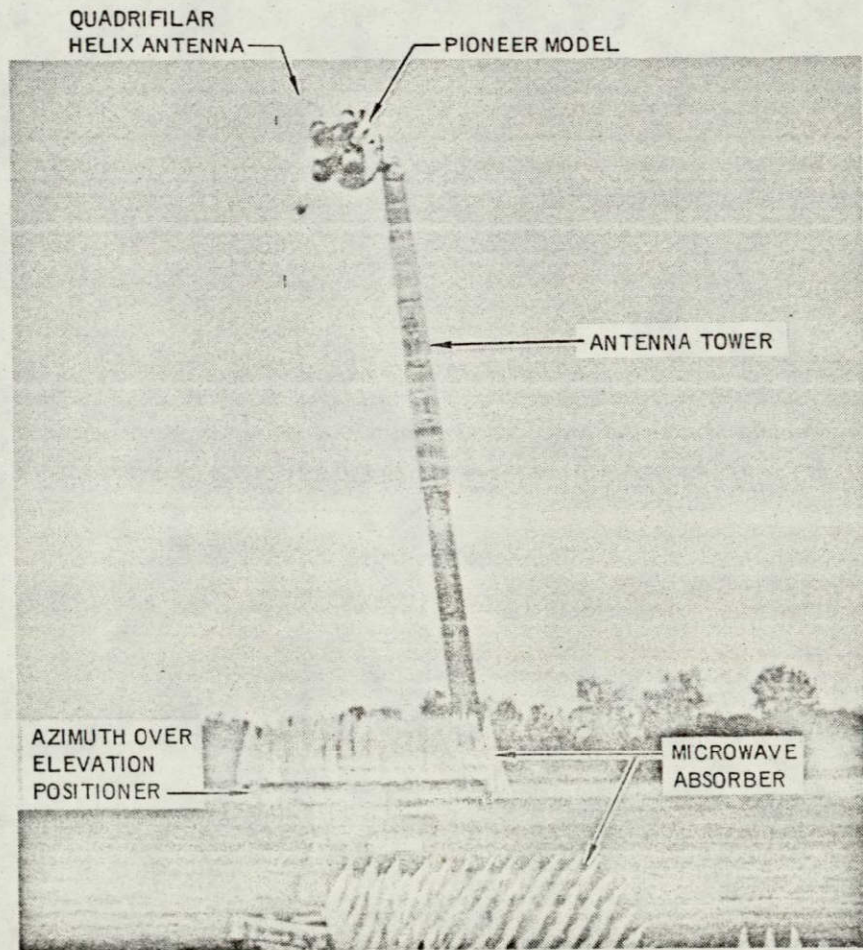
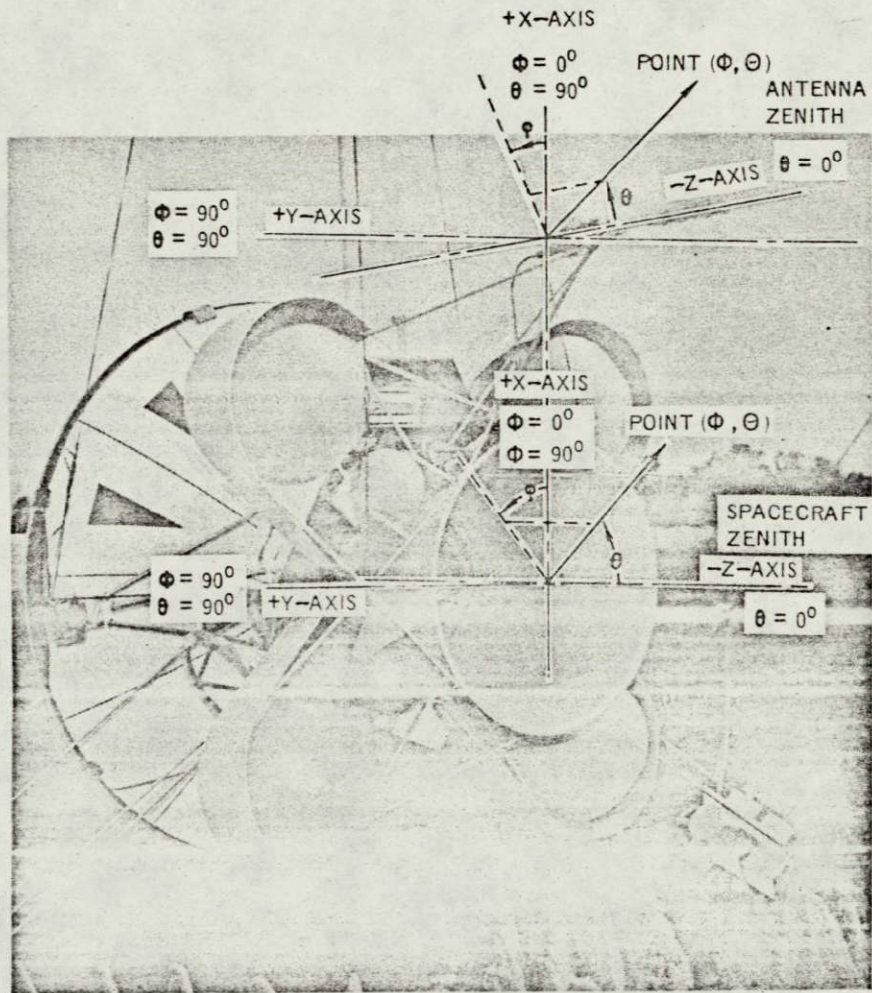


FIGURE 11

PIONEER SPACECRAFT TEST CONFIGURATION



NOTE: X, Y, Z-AXIS NOTATION CORRESPONDS TO
ACTUAL SPACECRAFT COORDINATES

FIGURE 12
COORDINATE SYSTEM FOR ANTENNA PATTERN MEASUREMENTS

ORIGINAL PAGE IS
OF POOR QUALITY

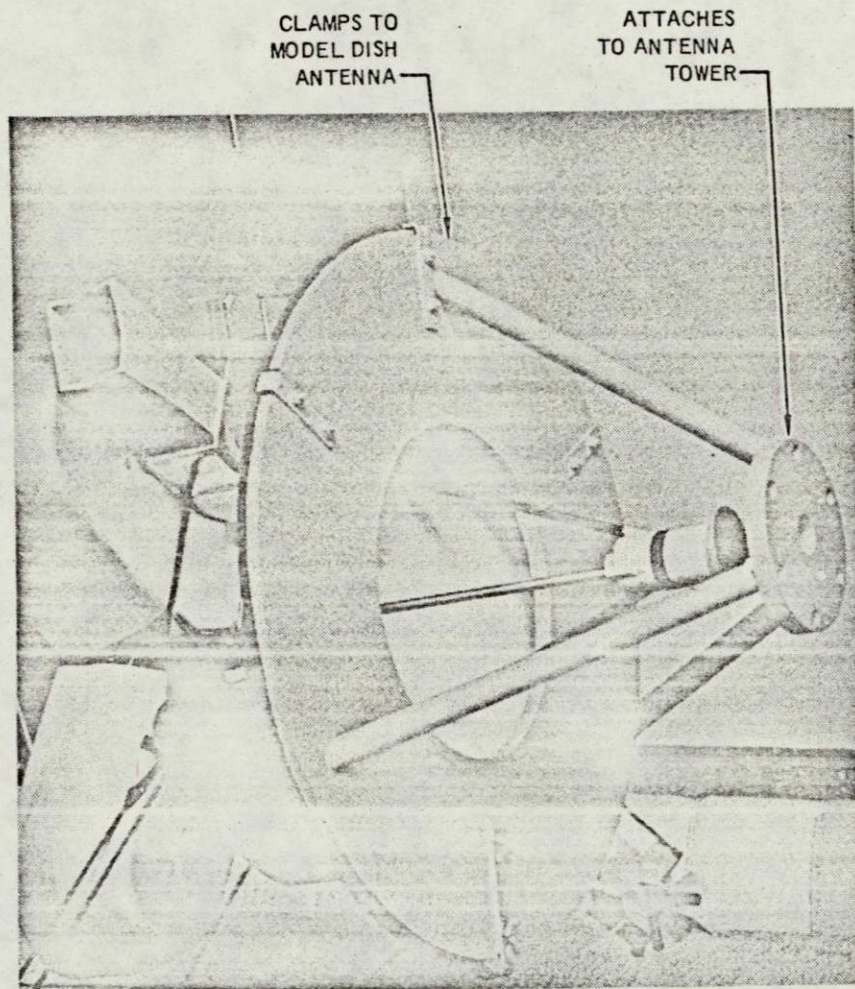


FIGURE 13
MODEL SPACECRAFT SUPPORT
FIXTURE FOR RADIATION PATTERN MEASUREMENTS

ORIGINAL PAGE IS
OF POOR QUALITY

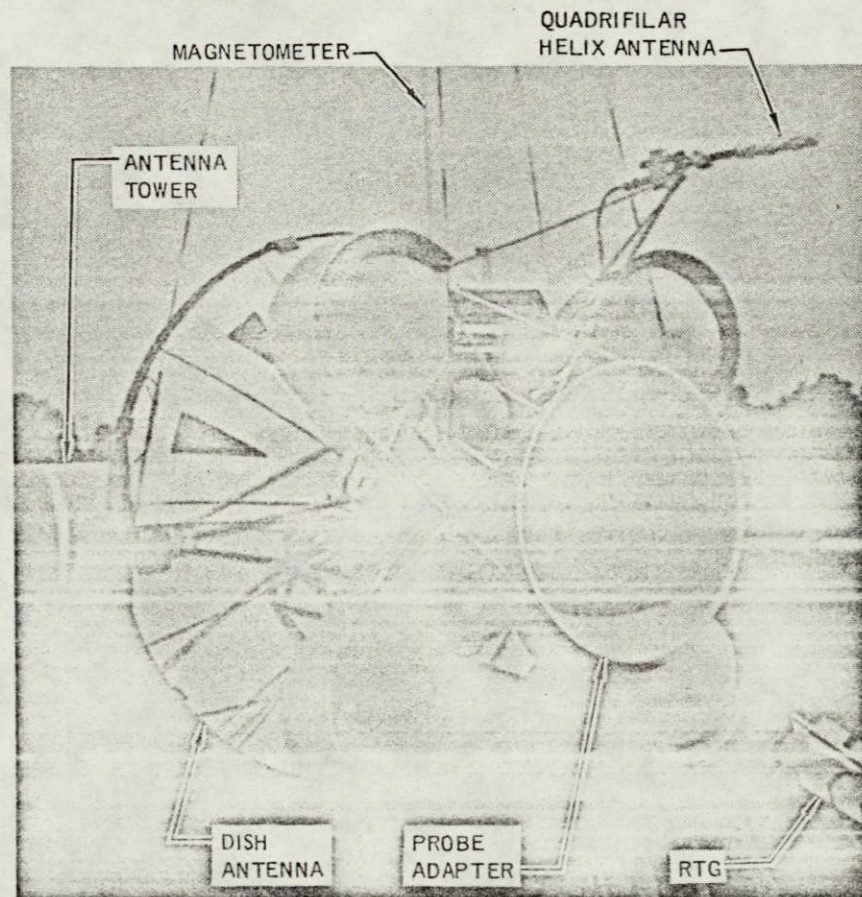


FIGURE 14
BASIC SPACECRAFT TEST CONFIGURATION

ORIGINAL PAGE IS
OF POOR QUALITY

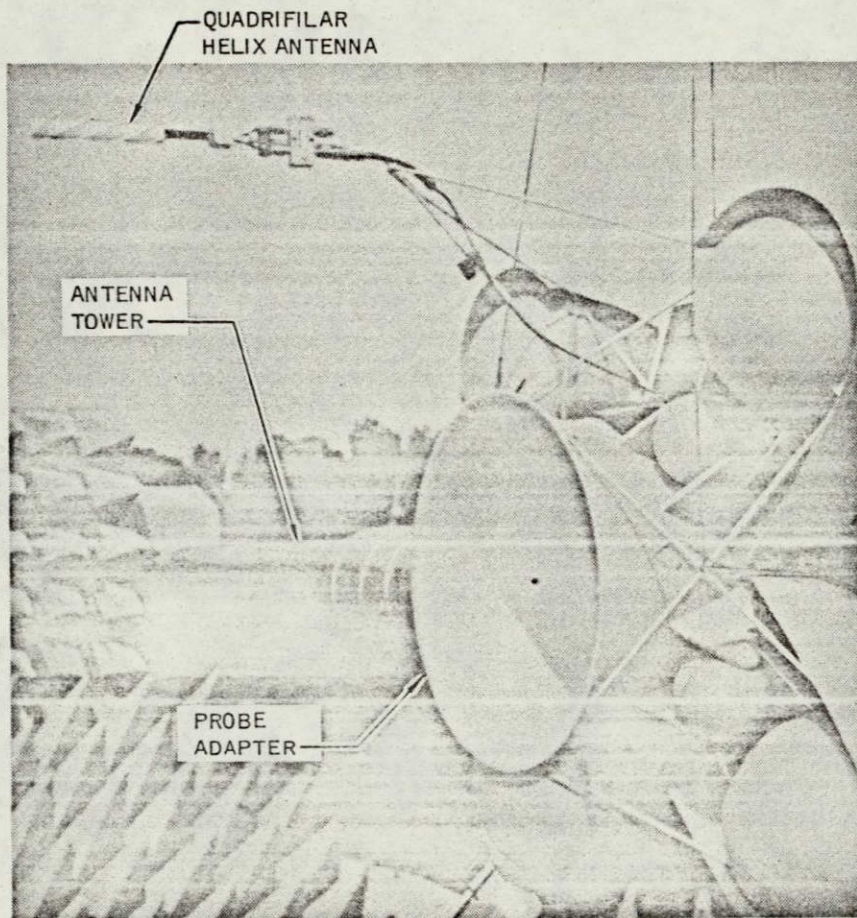


FIGURE 15
ANTENNA EXTENDED AXIALLY AFT OF POSITION
FOR BASIC TEST CONFIGURATION

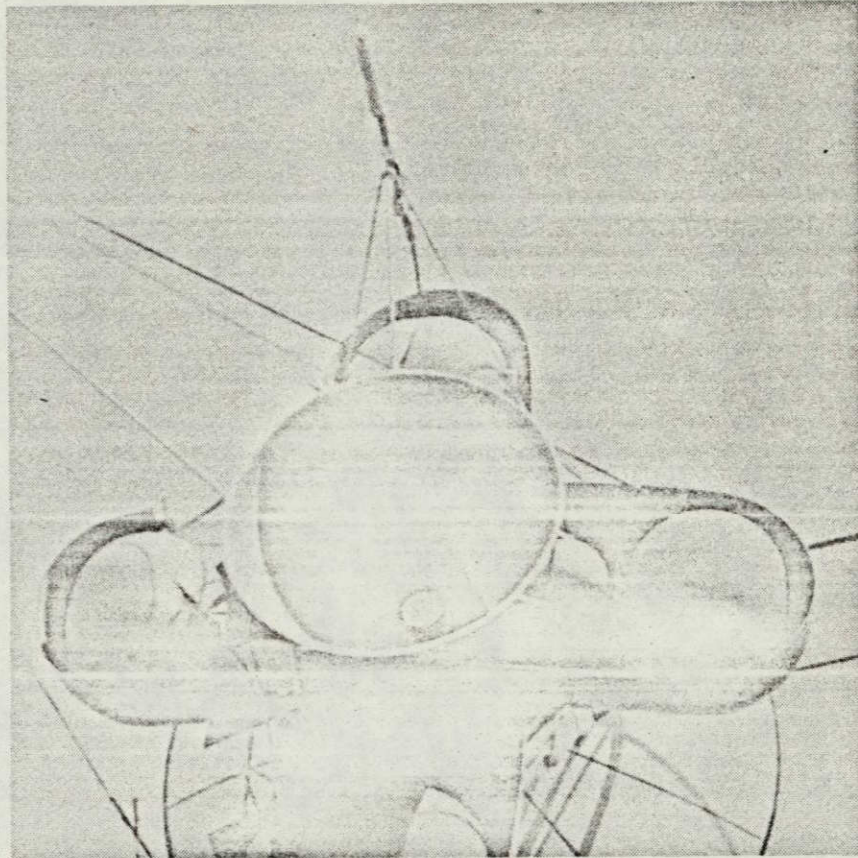


FIGURE 16
ANTENNA POSITION ROTATED
22.5° RELATIVE TO BASIC TEST CONFIGURATION

ORIGINAL PAGE IS
OF POOR QUALITY

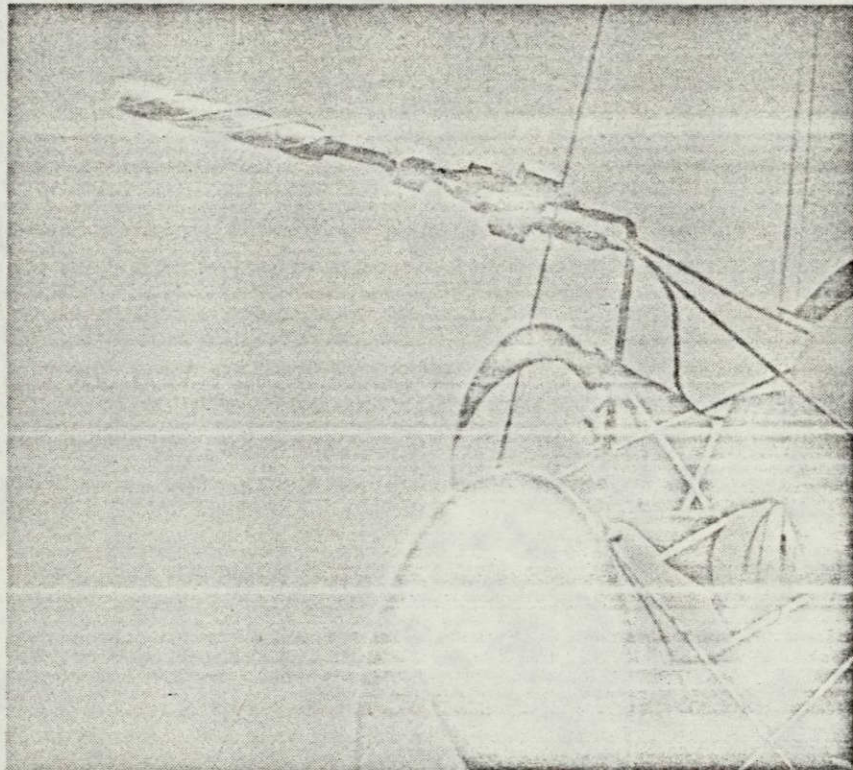


FIGURE 17
ANTENNA EXTENDED AXIALLY AFT FOR ROTATED POSITION

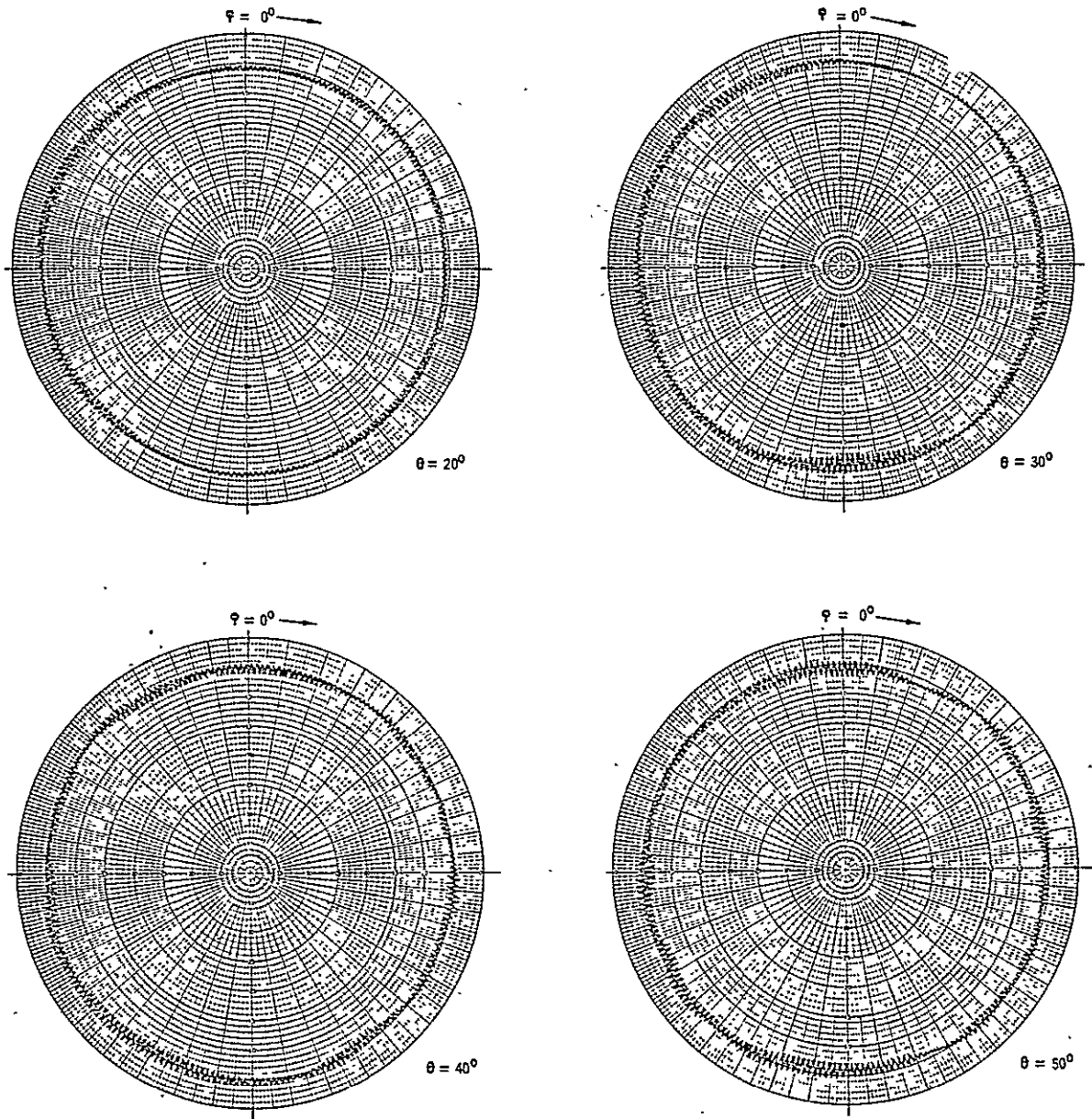


FIGURE 18 (Continued)

RADIATION PATTERNS FOR TEST CONFIGURATION NO. 1 - 2.2 GHz

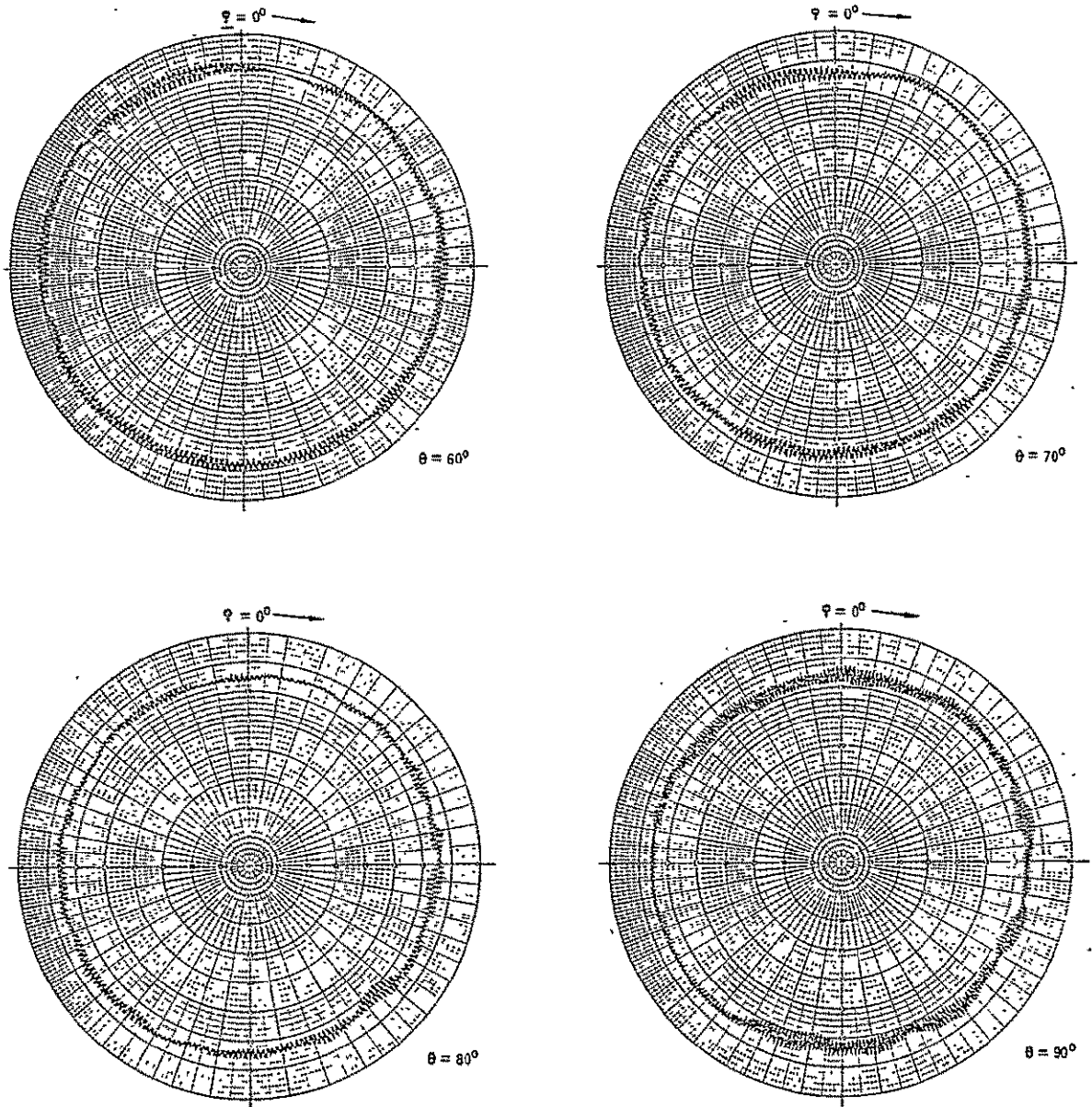


FIGURE 18 (Continued)

RADIATION PATTERNS FOR TEST CONFIGURATION NO. 1 - 2.2 GHz

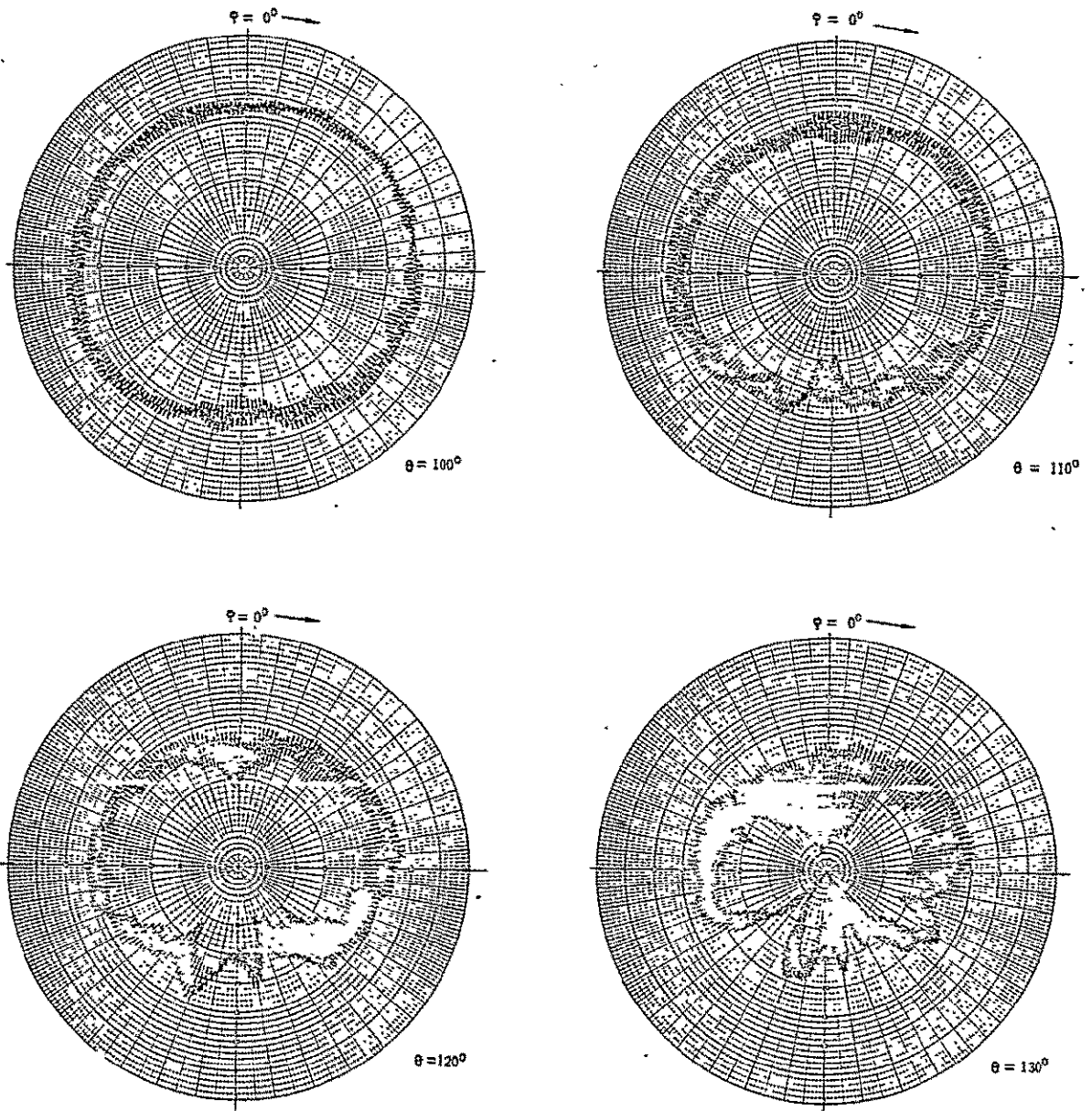


FIGURE 18 (Continued)
 RADIATION PATTERNS FOR TEST CONFIGURATION NO. 1 - 2.2 GHz

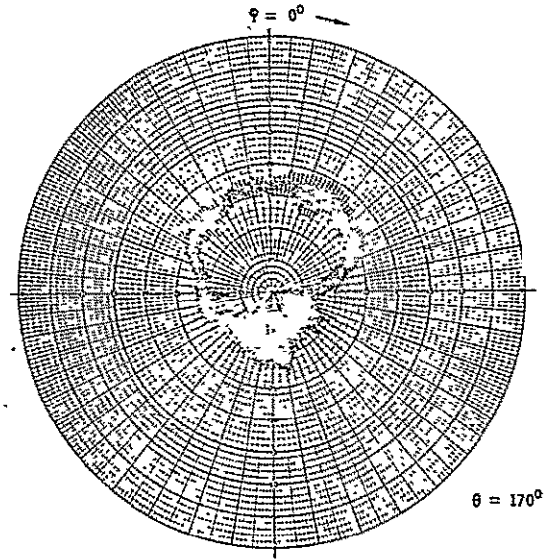
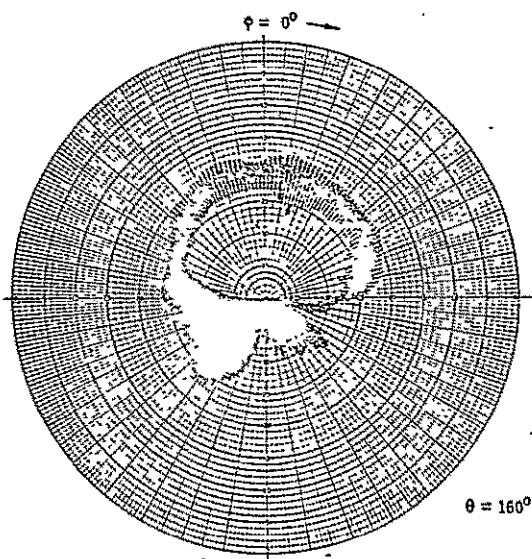
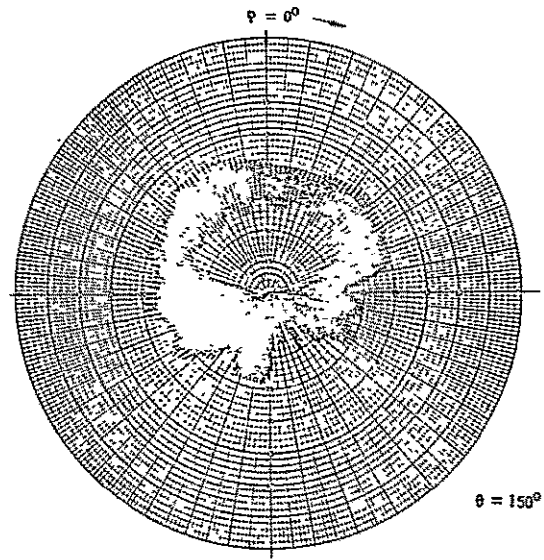
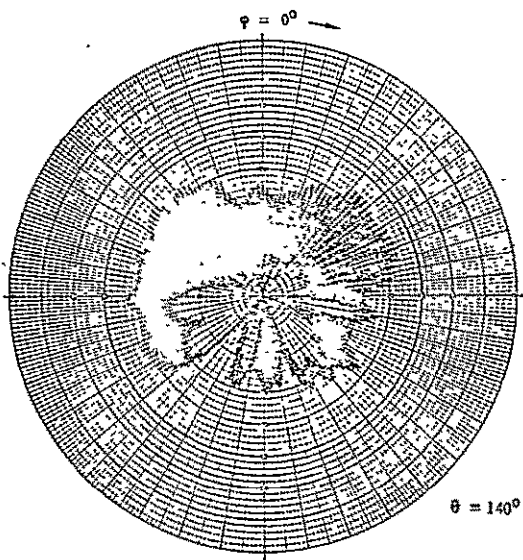


FIGURE 18 (Continued)
 RADIATION PATTERNS FOR TEST CONFIGURATION NO. 1 - 2.2 GHz

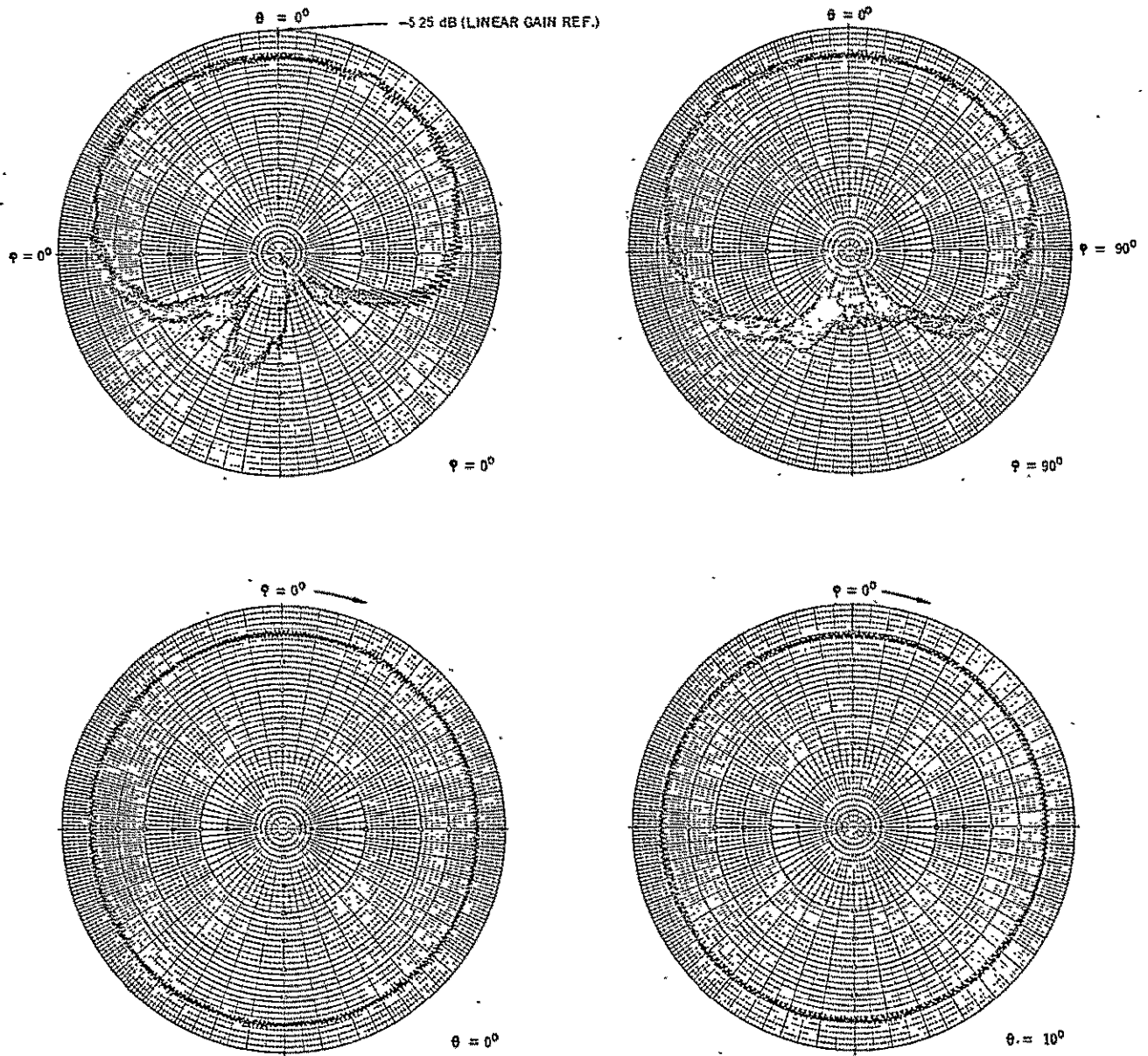


FIGURE 19
 RADIATION PATTERNS FOR TEST CONFIGURATION NO. 2. - 2.2 GHz

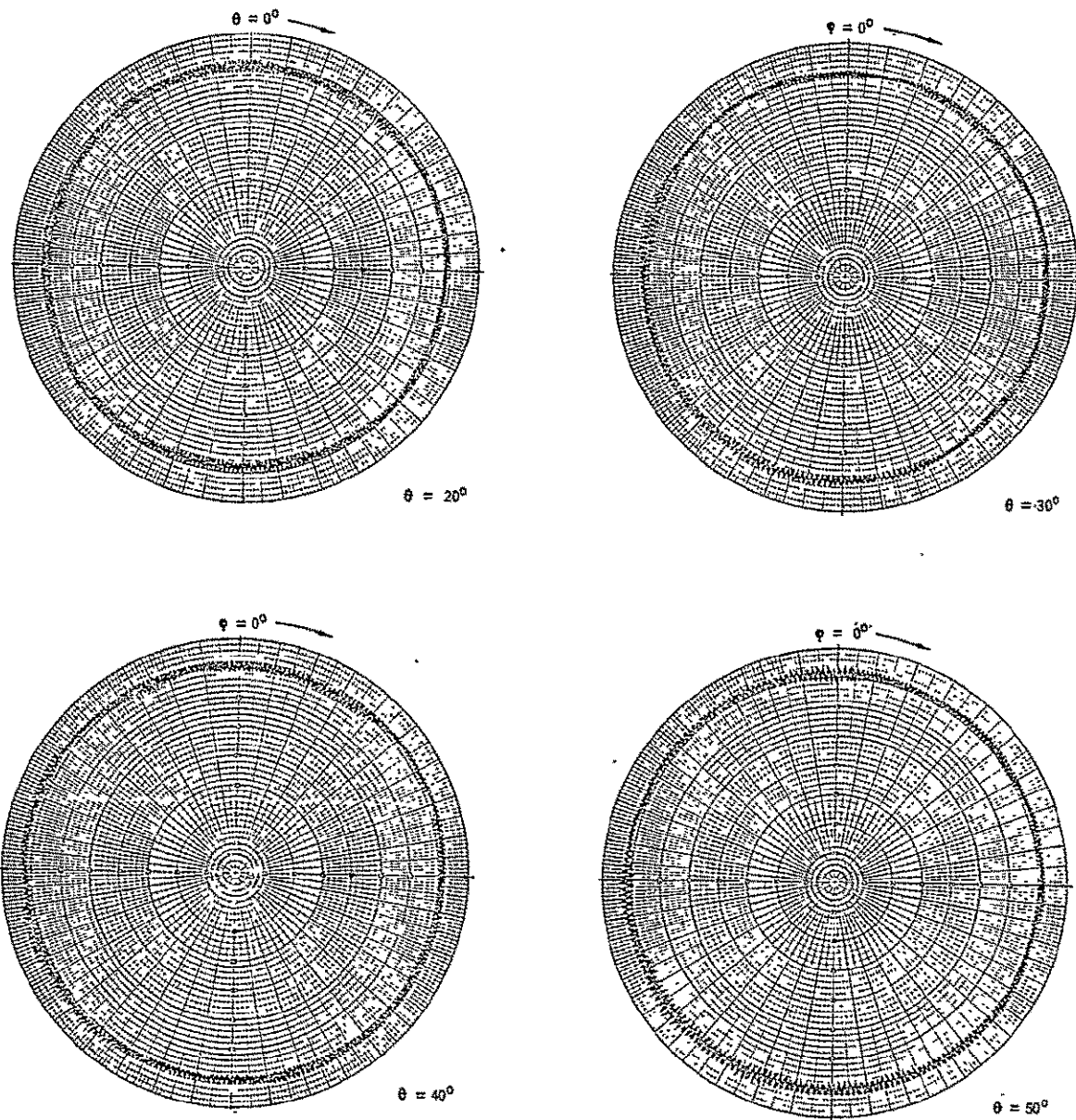


FIGURE 19 (Continued)
 RADIATION PATTERNS FOR TEST CONFIGURATION NO. 2 - 2.2 GHz

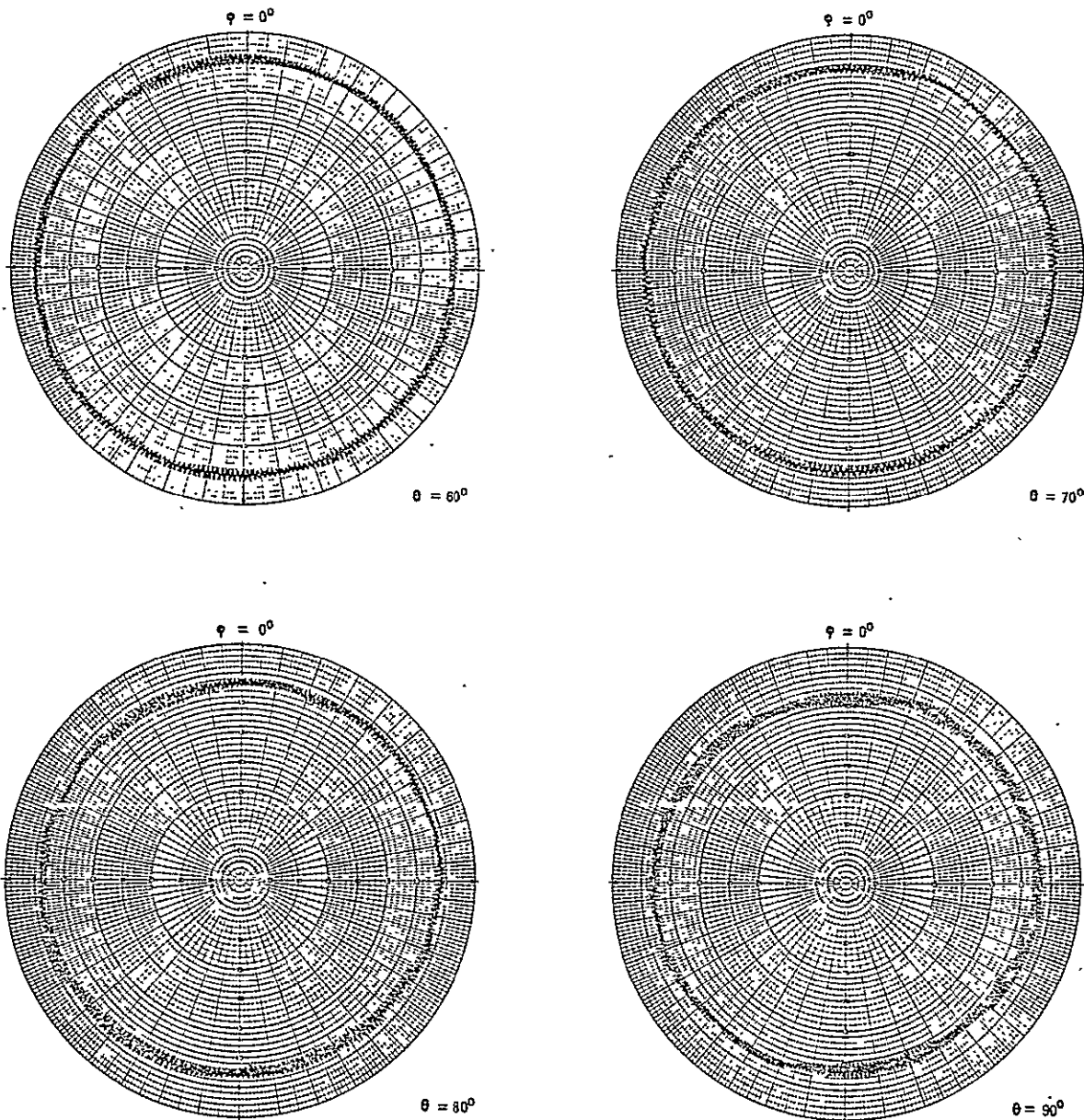


FIGURE 19 (Continued)
 RADIATION PATTERNS FOR TEST CONFIGURATION NO. 2 - 2.2 GHz

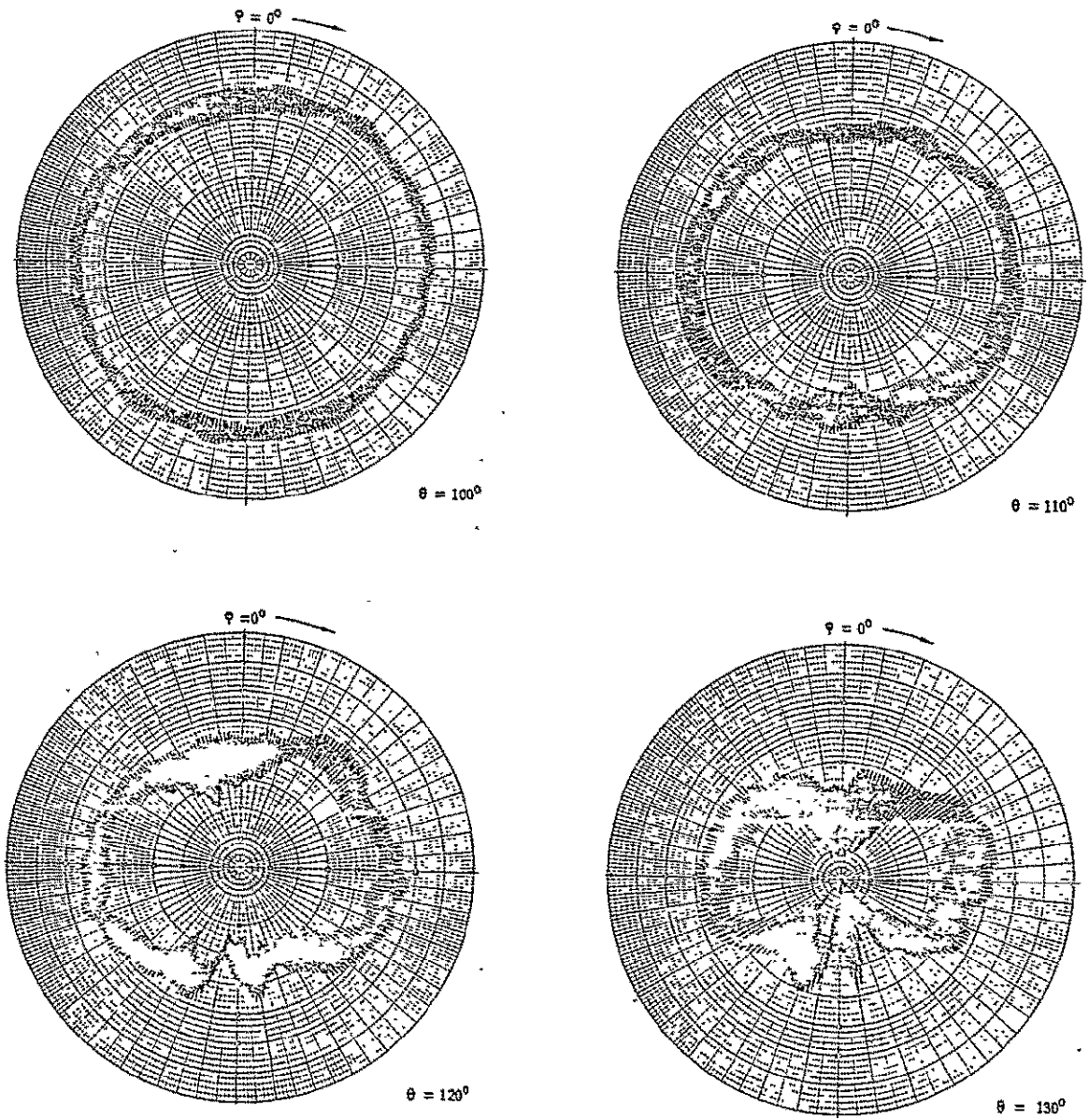


FIGURE 19 (Continued)
 RADIATION PATTERNS FOR TEST CONFIGURATION NO. 2 - 2.2 GHz

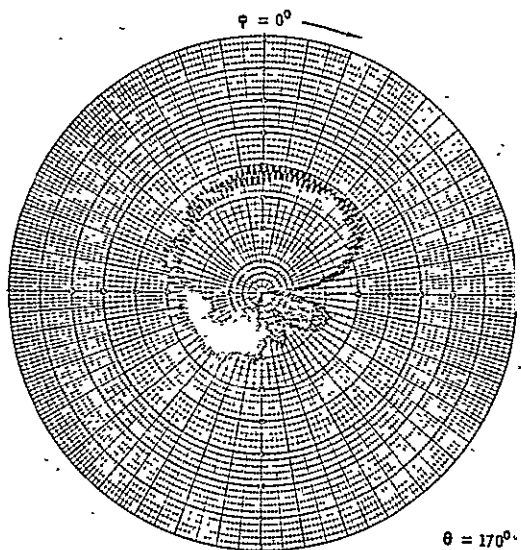
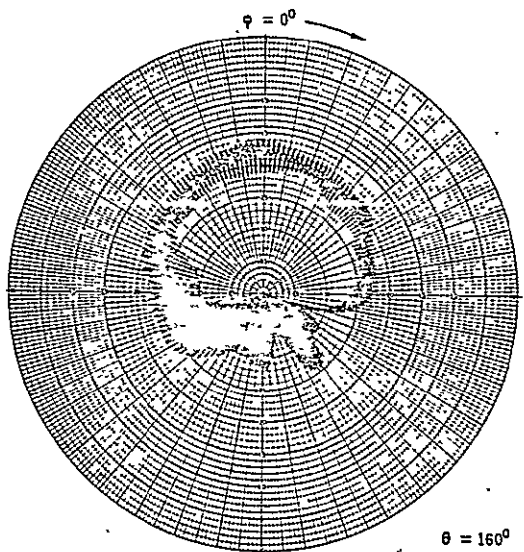
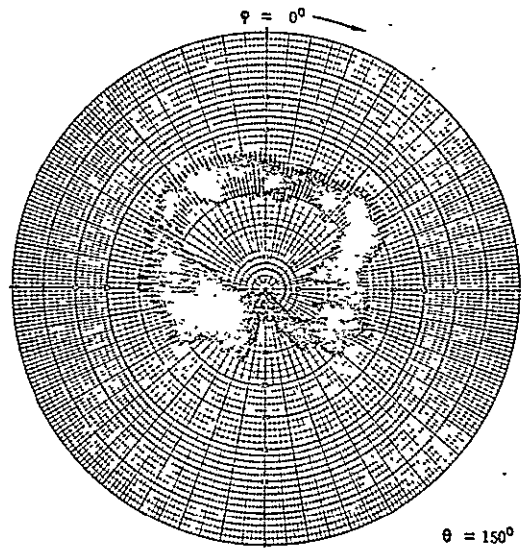
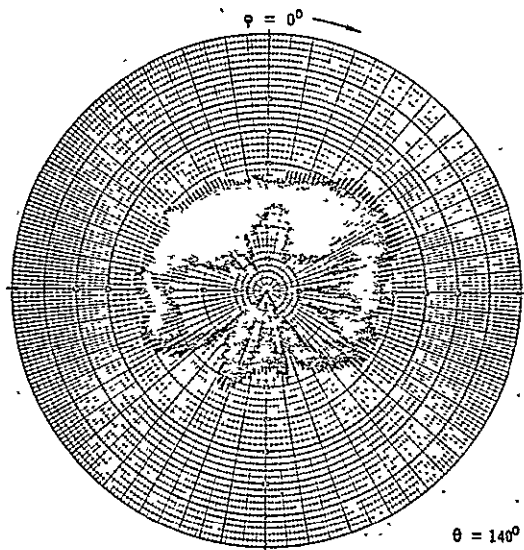


FIGURE 19 (Continued)
 RADIATION PATTERNS FOR TEST CONFIGURATION NO. 2 - 2.2 GHz

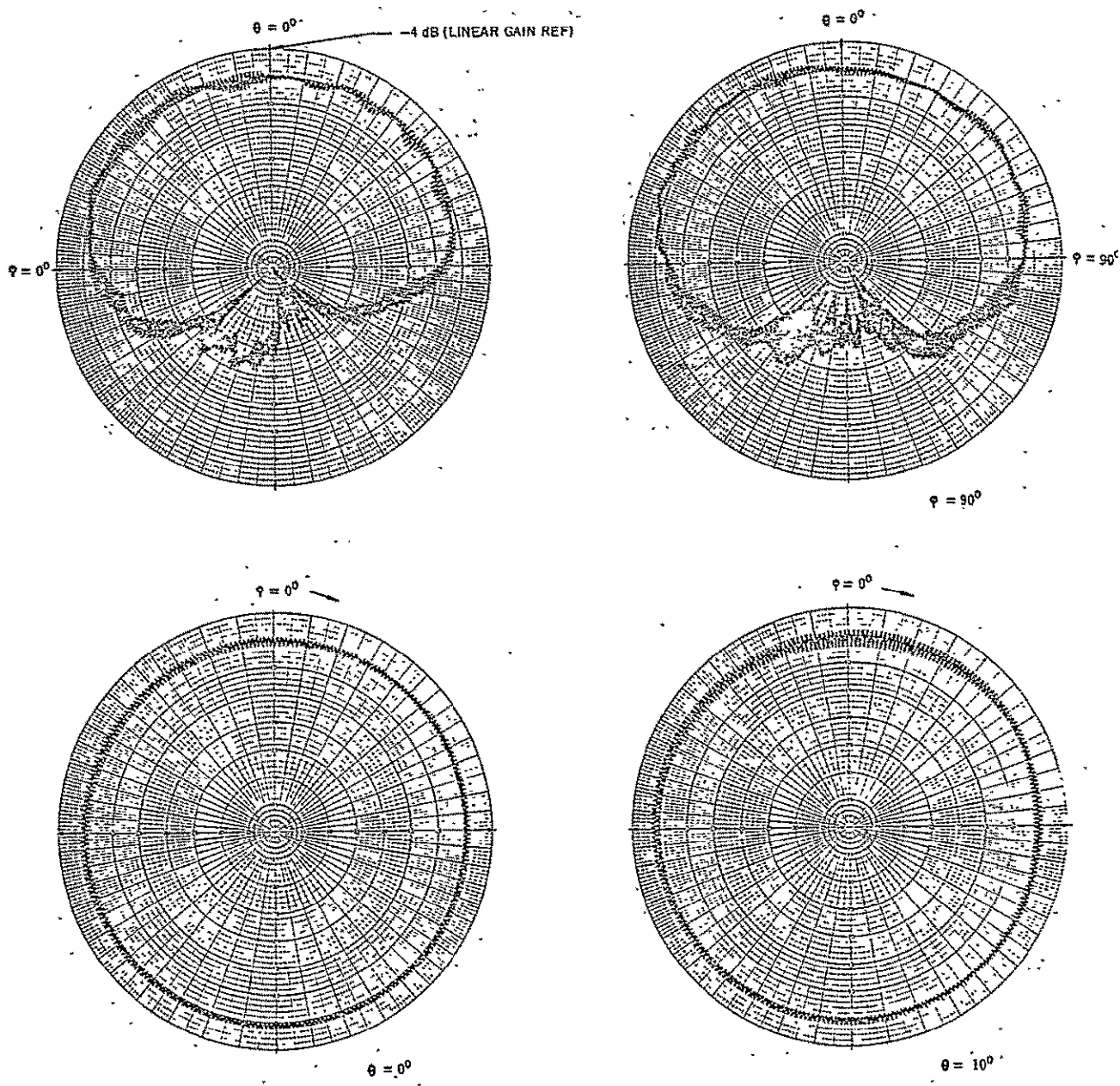


FIGURE 20
 RADIATION PATTERNS FOR TEST CONFIGURATION NO. 3 - 2.2 GHz

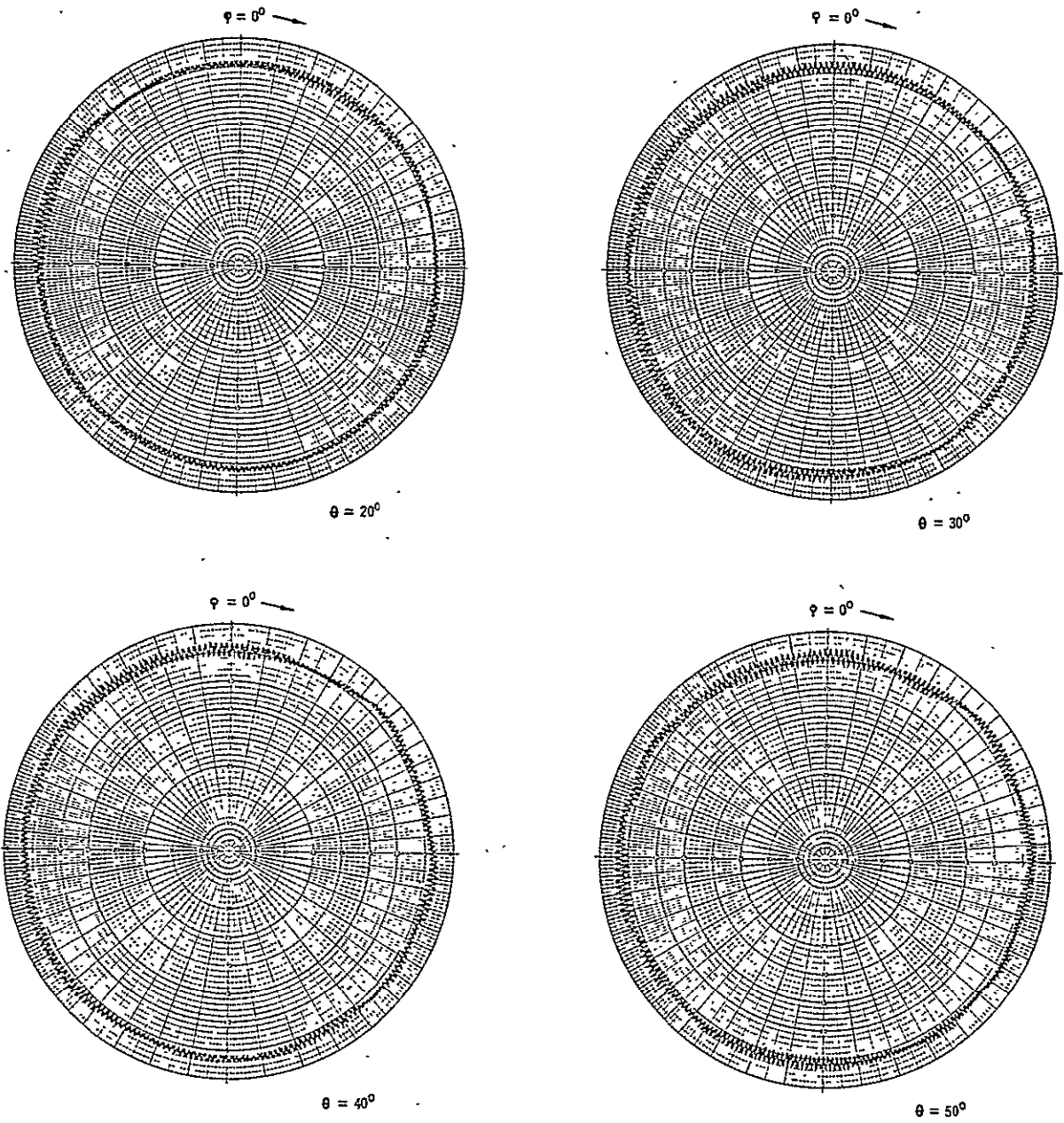


FIGURE 20 (Continued)
 RADIATION PATTERNS FOR TEST CONFIGURATION NO. 3 ~ 2.2 GHz

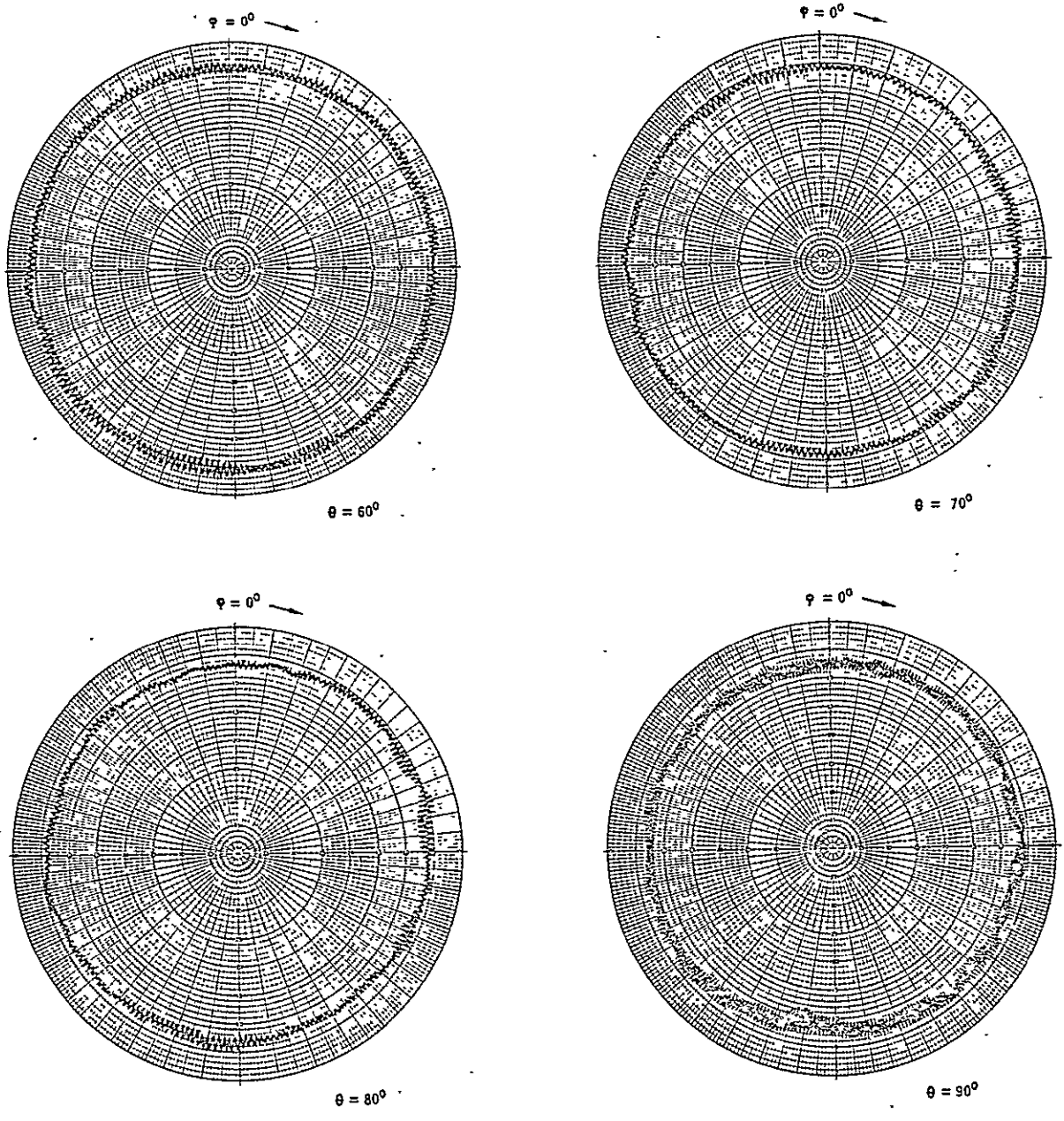


FIGURE 20 (Continued)
 RADIATION PATTERNS FOR TEST CONFIGURATION NO. 3 - 4.2 GHz

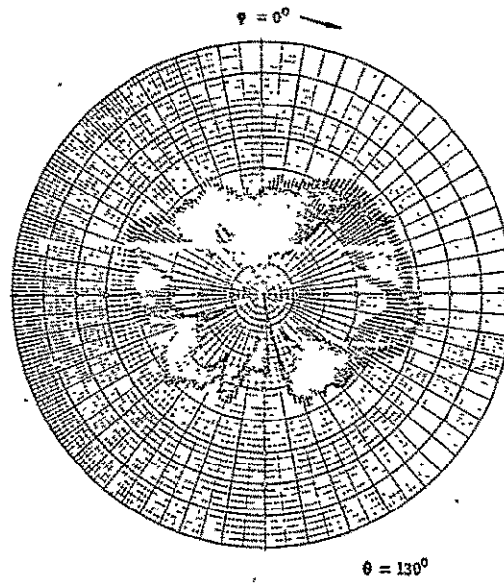
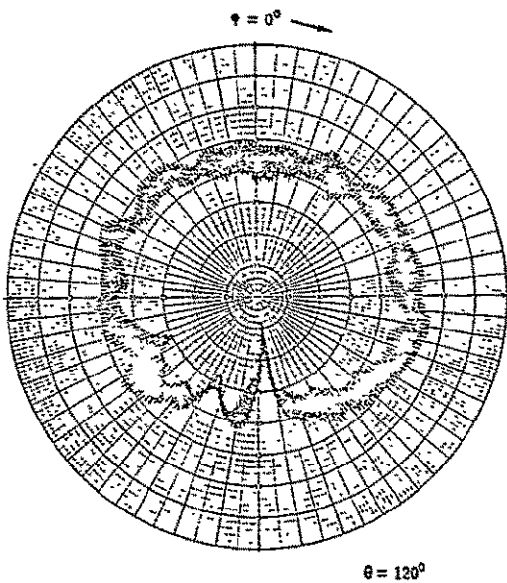
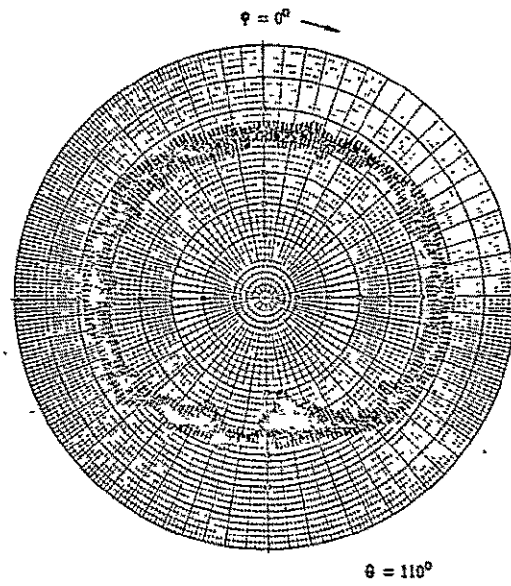
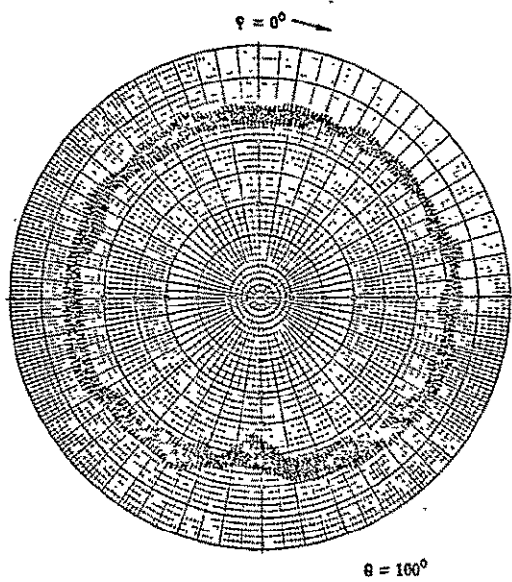


FIGURE 20 (Continued).
 RADIATION PATTERNS FOR TEST CONFIGURATION NO: 3 - 2.2 GHz

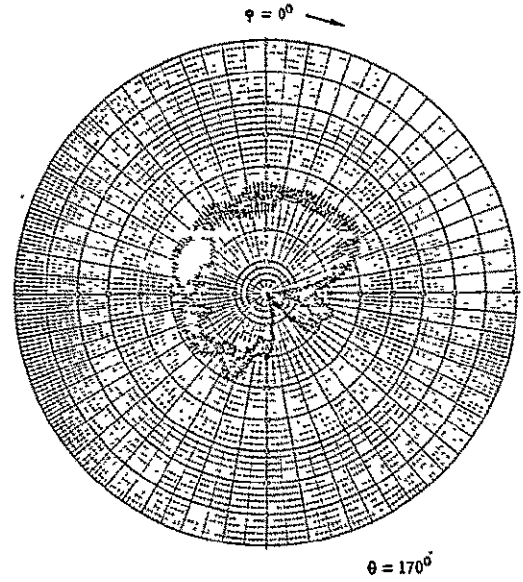
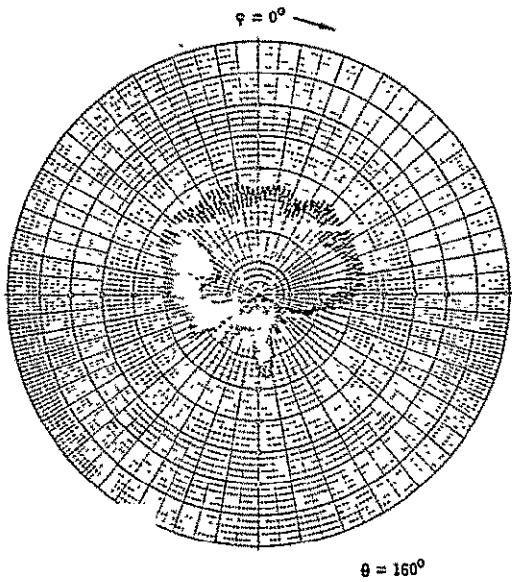
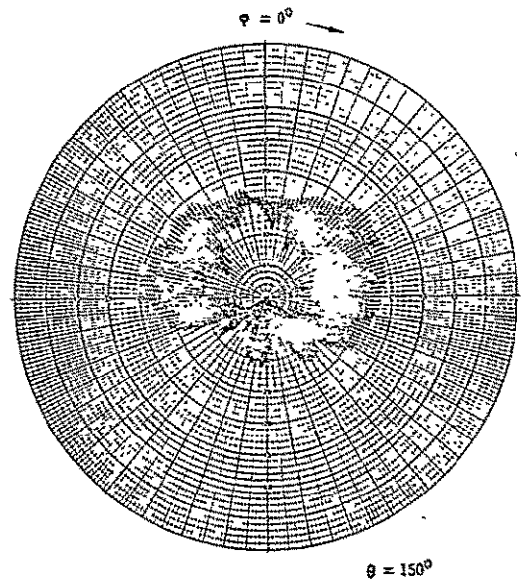
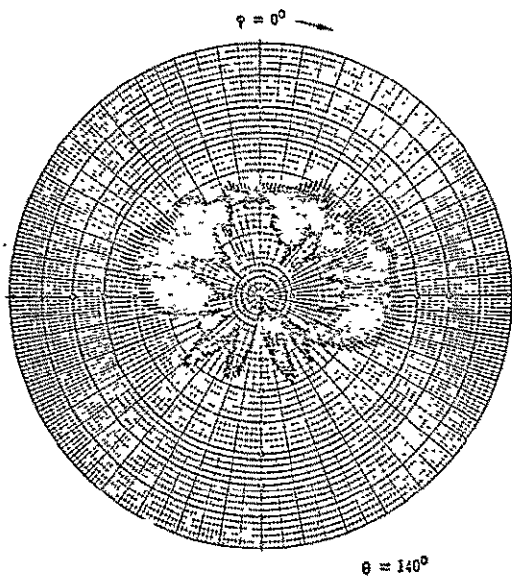


FIGURE 20 (Continued)
 RADIATION PATTERNS FOR TEST CONFIGURATION NO. 3 - 2.2 GHz

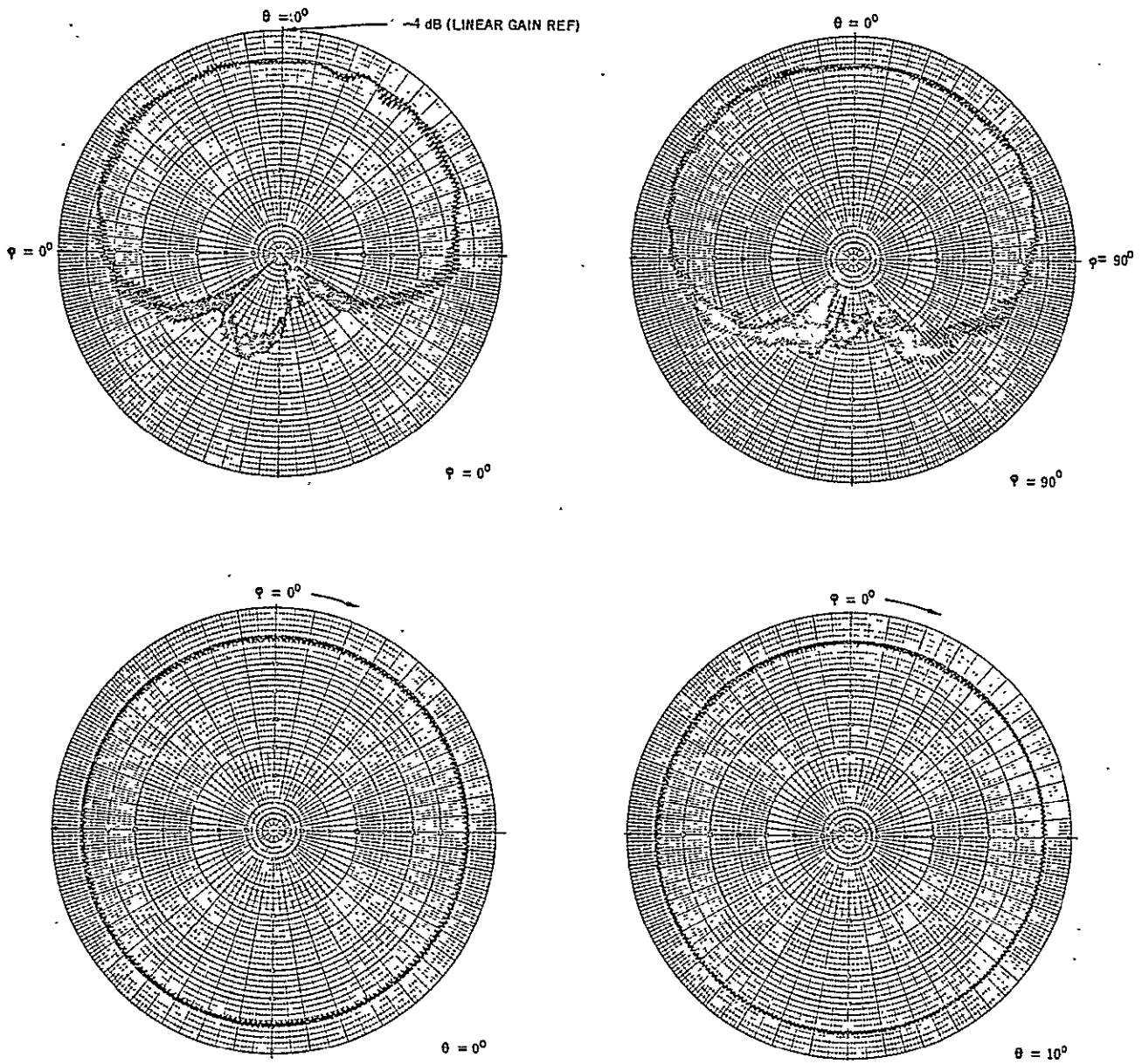


FIGURE 21
RADIATION PATTERNS FOR TEST CONFIGURATION NO. 4 - 2.2 GHz

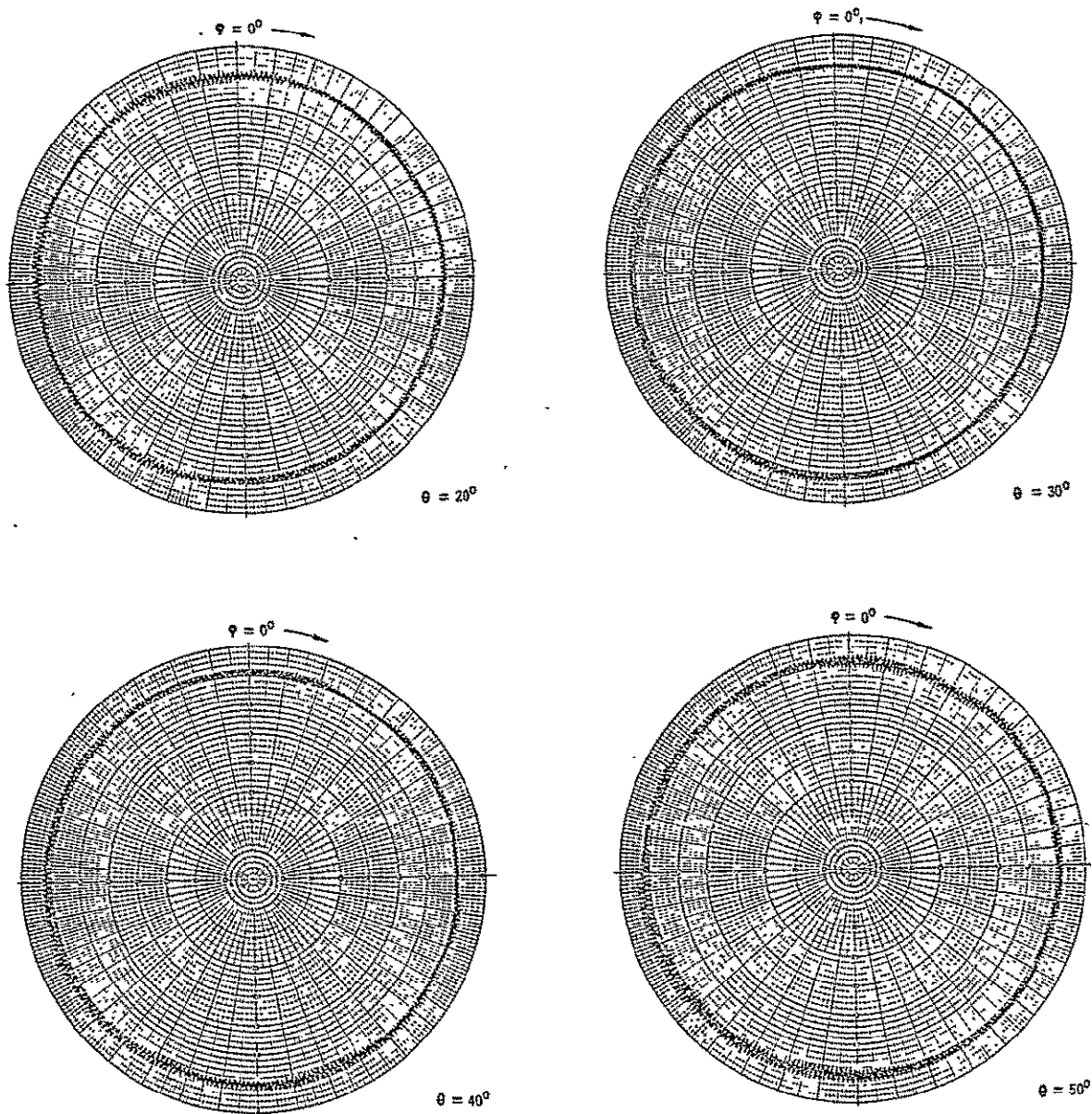


FIGURE 21 (Continued)
 RADIATION PATTERNS FOR TEST CONFIGURATION NO. 4 - 2.2 GHz

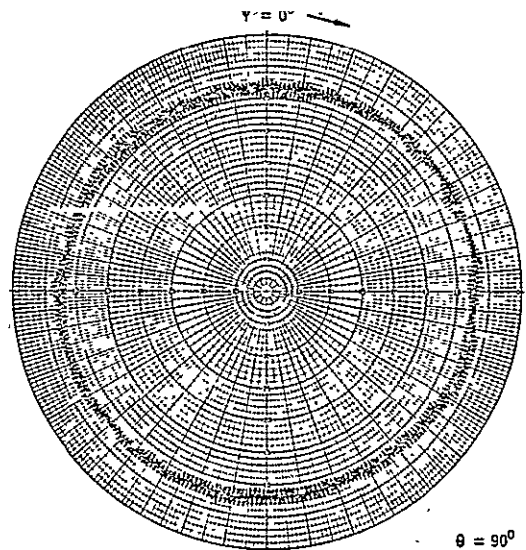
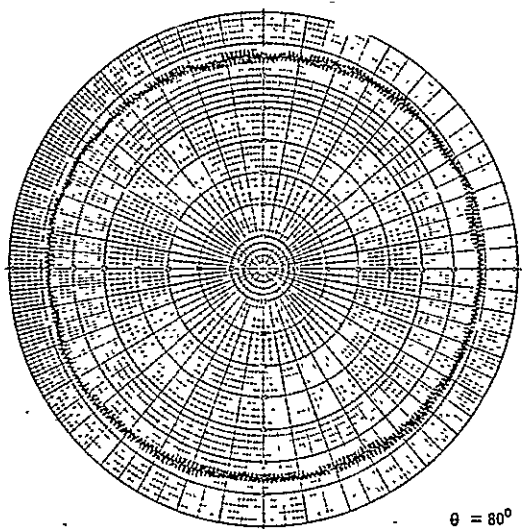
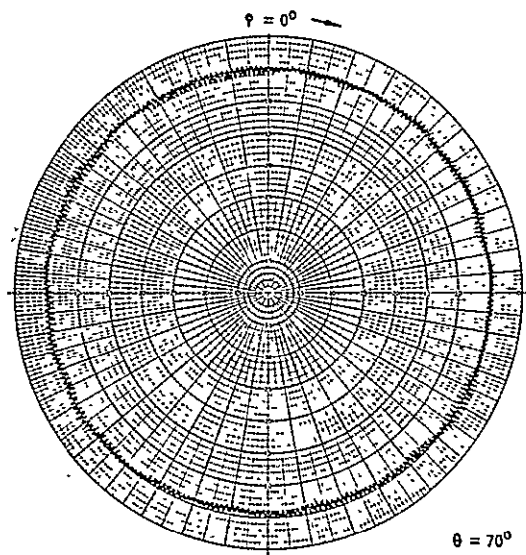
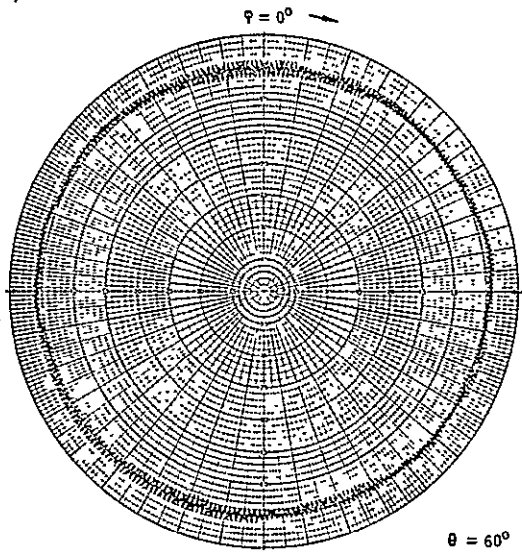


FIGURE 21 (Continued)
 RADIATION PATTERNS FOR TEST CONFIGURATION NO. 4 - 2.2 GHz

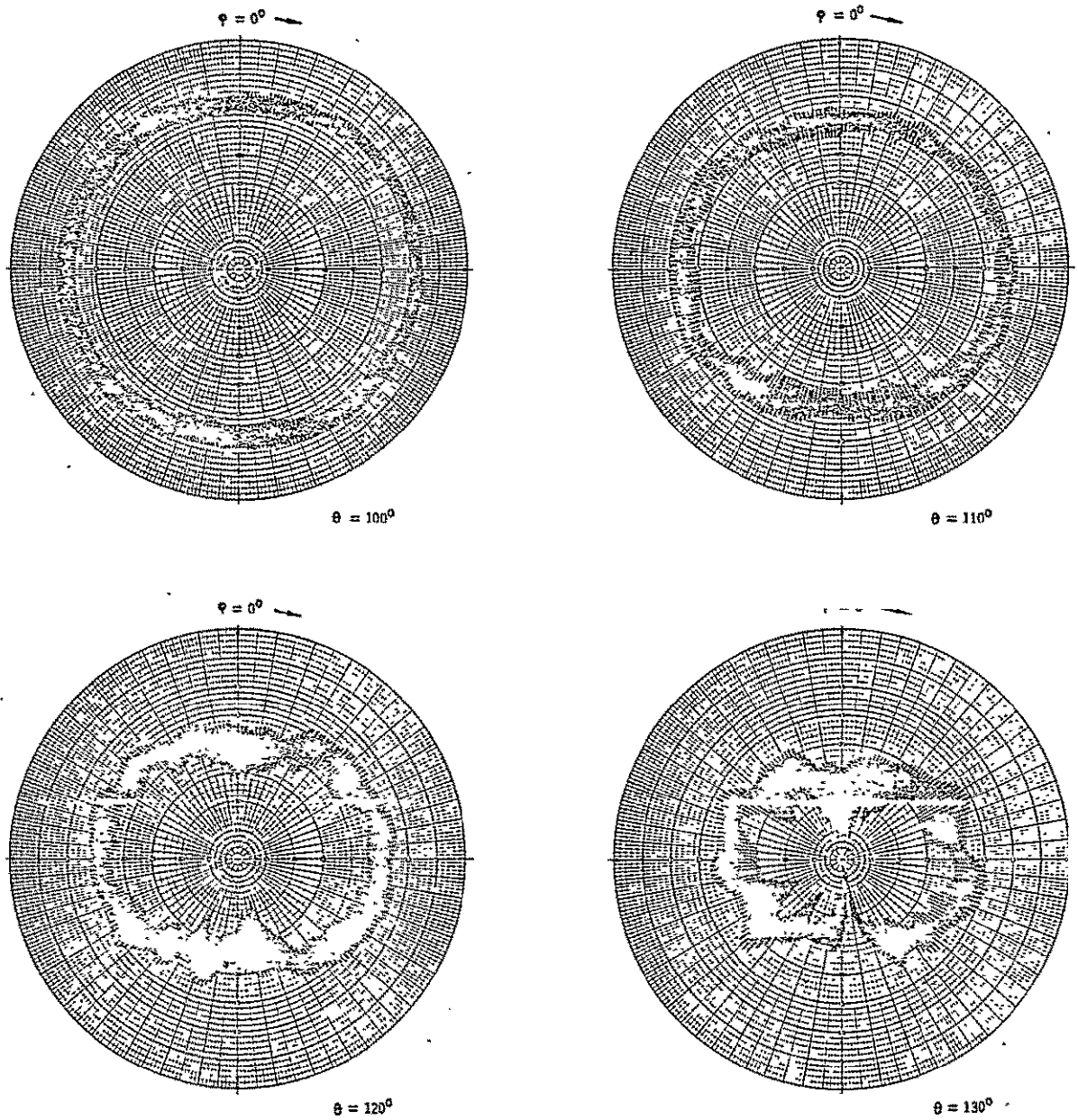


FIGURE 21 (Continued)

RADIATION PATTERNS FOR TEST CONFIGURATION NO. 4 - 2.2 GHz

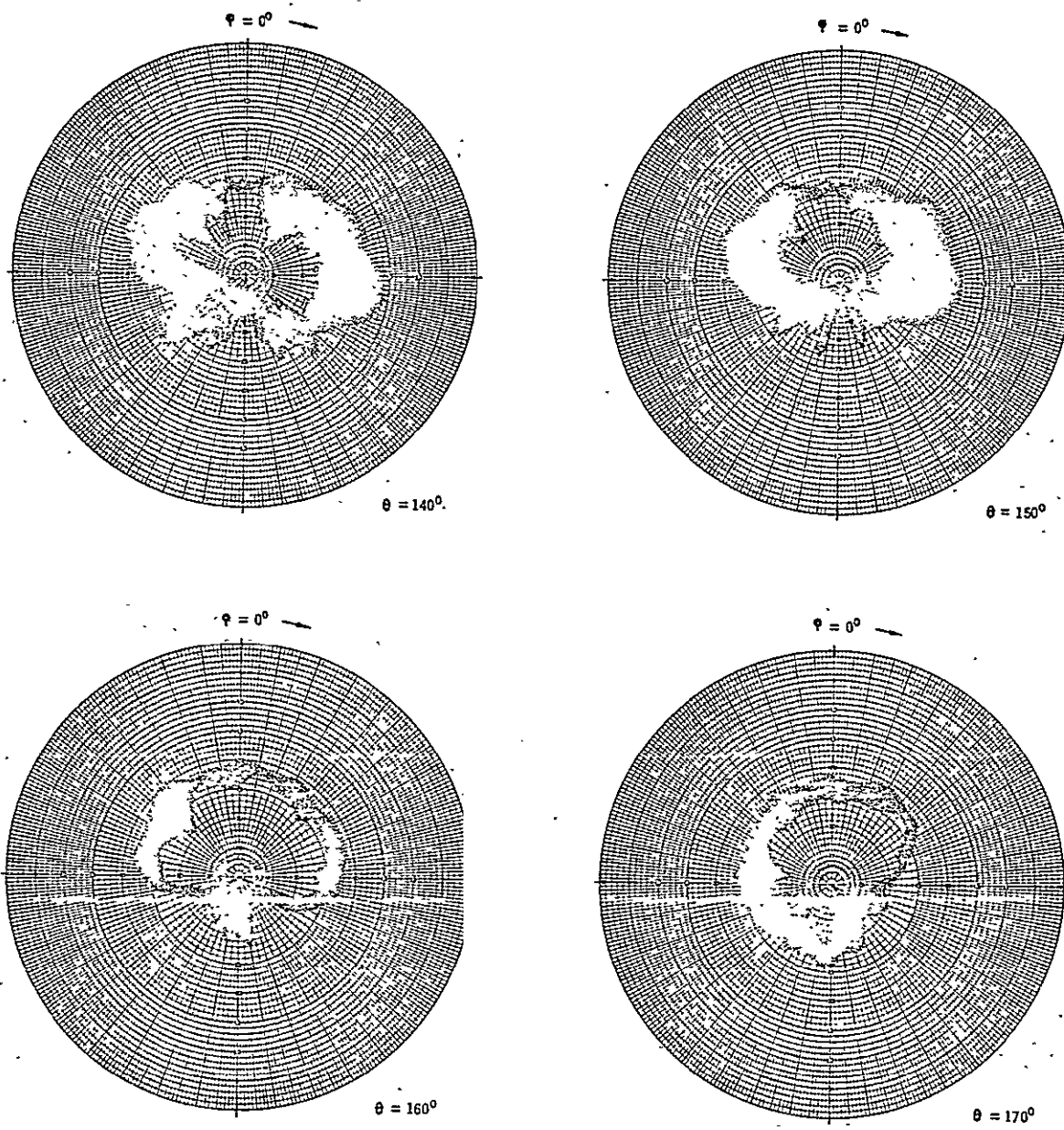


FIGURE 21 (Continued)
 RADIATION PATTERNS FOR TEST CONFIGURATION NO. 4 - 2.2 GHz

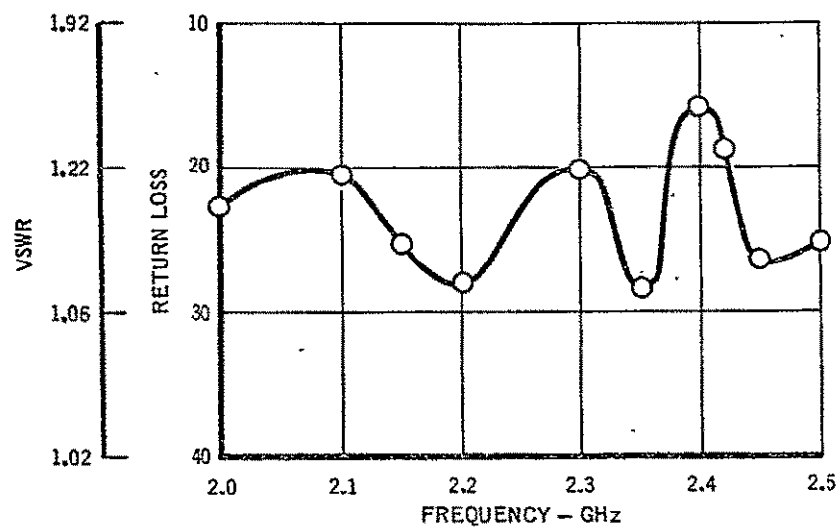


FIGURE 22

VSWR OF ANTENNA MOUNTED ON SPACECRAFT

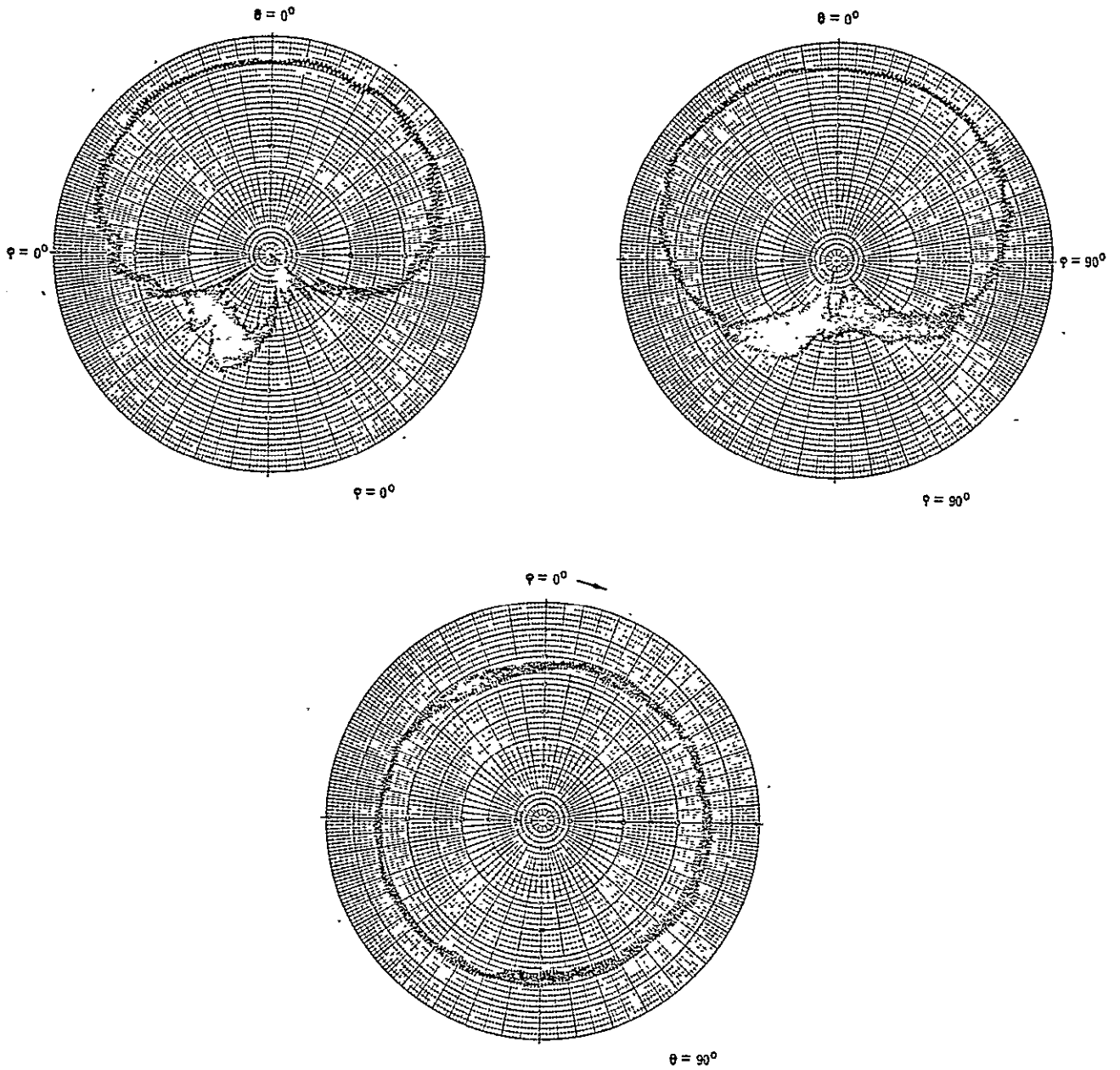


FIGURE 23
 RADIATION PATTERNS FOR BANDWIDTH EVALUATION - 20 GHZ

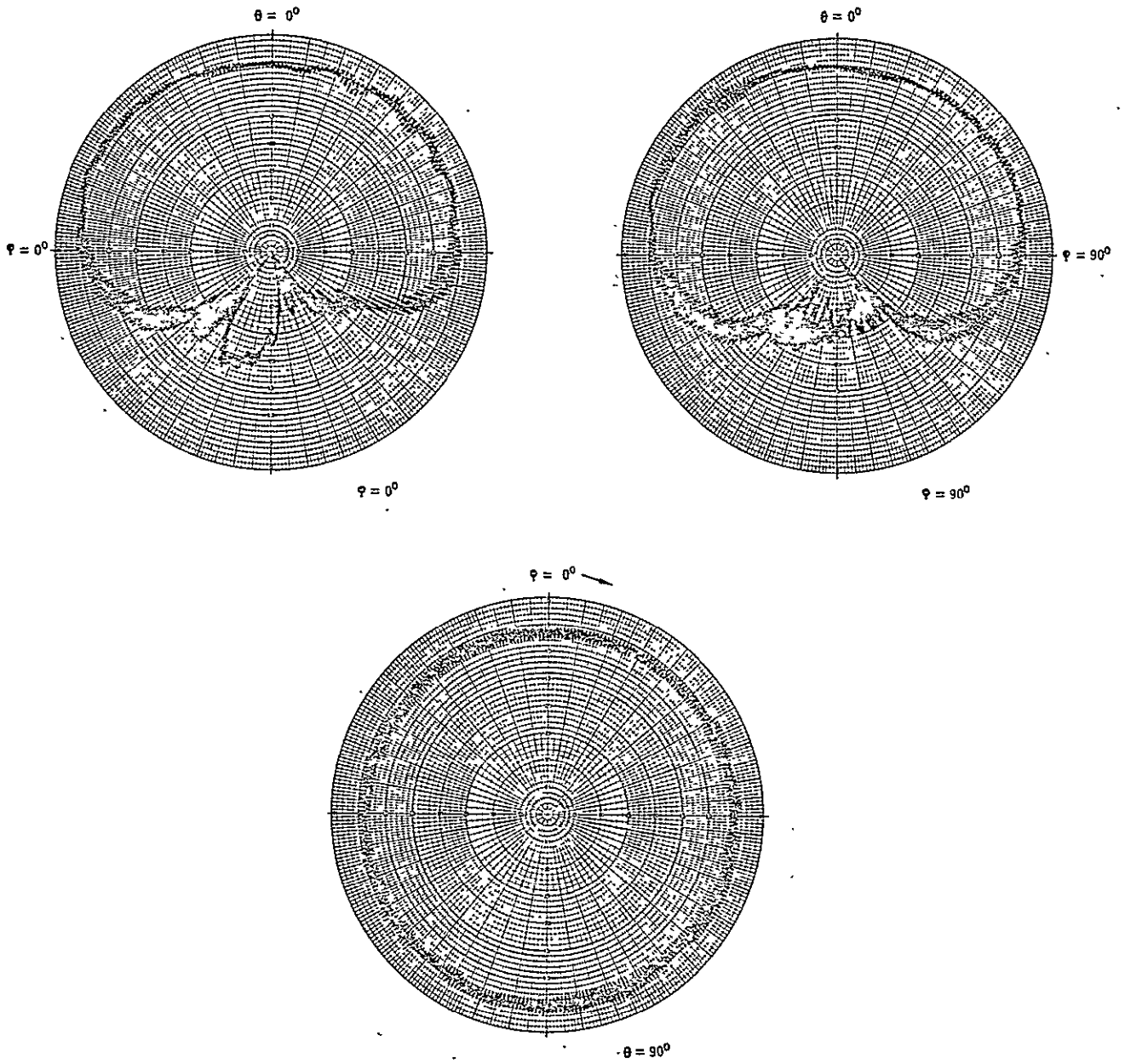


FIGURE 24
RADIATION PATTERNS FOR BANDWIDTH EVALUATION - 2.3 GHz

CONCLUSIONS

A quadrifilar helix antenna has been selected for the Pioneer spacecraft. A 1/4 scale model of the quadrifilar helix antenna was constructed and tested. The results of these tests, radiation pattern and VSWR measurements, show that this antenna has excellent pattern symmetry, 1.5 dB peak to peak compared to a goal of 1 dB from $\theta = 0^\circ$ to $\theta = 90^\circ$ and an axial ratio maximum of 2.5 dB over the same angular region. Over much of this region the axial ratio is 0.5 dB or less. To improve on these results, it is believed that use of special precision tooling would be required during the construction process to control the geometry of the quadrifilar helix elements more precisely. Based on these test results, it can be concluded that the model antenna performance is ideal for evaluating the effects of the spacecraft on the axial symmetry of a receiving antenna.

The results of the radiation pattern measurements show that the antenna location is not critical. Over the aft hemisphere ($\theta = 0^\circ$ to $\theta = 90^\circ$) the worst pattern symmetry is 2.5 dB peak to peak and the maximum axial ratio is 3 dB or less for all of the configurations tested. However, the pattern symmetry and axial ratio of the radiation patterns is improved with the antennas located as far from the spacecraft as possible.

The test results show that the spacecraft has no significant effect on the antenna impedance (VSWR) or bandwidth. Based on the test results obtained during this study, it is concluded that the quadrifilar helix antenna will provide radiation patterns with good symmetry and low axial ratios at spacecraft look angles over the aft hemisphere. The peak circular gain of the quadrifilar helix antenna, when scaled to 550 MHz, should be about 2.2 dB based on an expected efficiency of 71% (-1.5 dB) at the larger size.

REFERENCES

1. Hinrichs, C. A.: McDonnell Douglas Astronautics Company-East: "Preentry Communications Study for Outer Planets Atmosphere Entry Probe", NASA CR 137876, May 1976.
2. TRW Systems Group: Saturn Uranus Atmospheric Entry Probe Mission Space-Craft System Definition Study. Final Report, Contract NAS 2-7297. 15 July 1973.
3. Kilgus, C. C.: "Multielement Fractional Turn Helices", IEEE Transactions on Antennas and Propagation, Vol. AP-16, July 1968, pp 499-501.
4. Kilgus, C. C.: "Resonant Quadrifilar Helix", IEEE Transactions on Antennas and Propagation, Vol. AP-17, May 1969, pp 349-351.
5. Kilgus, C. C.: "Resonant Quadrifilar Helix Design", Microwave Journal Volume 13-12, December 1970, pp 49-54.
6. Kilgus, C. C.: "Spacecraft and Ground Station Applications of the Resonant Quadrifilar Helix", Digest of the 1974 International IEEE/AP-S Symposium, June 1974, pp 75-77.
7. Bucker, R. W., and Rickert, H. H.: "An S-Band Resonant Quadrifilar Antenna for Satellite Communication", Digest of the 1974 International IEEE/AP-S Symposium, June 1974, pp 78-82.
8. Kilgus, C. C.: "Shaped-Conical Radiation Pattern Performance of the Backfire Quadrifilar Helix", IEEE Transactions on Antennas and Propagation, AP-23, May 1975, pp 392-396.
9. Domer, F. R.: "Two-Element Quadrifilar Array, Naval Research Laboratory, NRL Report 7661, 8 March 1974.
10. Frank, P. D.: Philco Ford Corporation, "Viking Orbiter 1975 Antenna Subsystems, Relay Antenna", Volume 3, JUP Subcontract No. 953379, 15 February 1974.
11. Roberts, W. K.: "A New Wide-Band Balun", Proceedings of the IRE, pp 1628-1631, December 1957.
12. Jasik, H. (Editor): Antenna Engineering Handbook, McGraw-Hill Book Company, New York, 1961, pp 31-22 - 31-25.
13. Shields, M. W.: "Final Report on SAS-C S-Band Antenna" Applied Physics Laboratory, Memo No. S2T-4-123, 31 January 1975.
14. C. C. Kilgus: Private Communication.

~~RECEIVING PAGE BLANK NOT FILMED~~

ACKNOWLEDGEMENTS

The author expresses his appreciation to E. D. McKee and R. M. Ousley of the McDonnell Aircraft Company Microwave Antenna Laboratory Staff for the fabrication and detailed modifications to the quadrifilar helix antenna model and the radiation pattern and impedance measurements.

REPRODUCING PAGE BLANK NOT FILMED